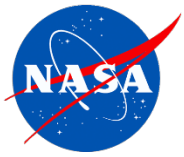

Spitzer Space Telescope Handbook

Spitzer Heritage Archive Documentation

Version 3.0, 8 January 2021

Table of Contents

Document History

Version	Comments
Version 3.0 Release: 8 January 2021	Added the warm mission, verb tenses
Version 2.1 Release: 8 March 2013	Minor updates to text in section 2.2.4
Version 2.0 Release: 1 April 2011	Final minor updates to text.
Version 1.1 Release: 5 March 2010	Minor text updates; first HTML version.
Version 1.0 Release: 9 February 2010	Initial release, PDF only.

Chapter 1. Introduction

1.1 Document Purpose and Scope

The Spitzer Telescope Handbook is one of a series of documents that explain the operations of the Spitzer Space Telescope and its three science instruments, the data received from the instruments and the processing carried out on the data. The Spitzer Space Telescope Handbook gives an overview of the entire Spitzer mission and it explains the operations of the observatory, while the other three handbooks document the operation of, and the data produced by the individual instruments (IRAC, IRS and MIPS). The Handbook is intended to provide information about the Spitzer mission and the observatory itself, including a historical review of the project, a description of the science and spacecraft operations, pointing and tracking capabilities, cross-calibration of the instruments, and the data archive. For detailed information about the science instruments and the data they produced, the reader is encouraged to consult the three Instrument Handbooks.

The science products from the Spitzer Space Telescope are available from the Spitzer Heritage Archive via the NASA/IPAC Infrared Science Archive (IRSA) at: http://sha.ipac.caltech.edu/applications/Spitzer/SHA.

1.2 How to Contact Us

A broad collection of information relating to the Spitzer mission is available on the IRSA web site at http://irsa.ipac.caltech.edu/data/SPITZER/docs/. You may also contact us at the Helpdesk: http://irsa.ipac.caltech.edu/data/SPITZER/docs/spitzerhelpdesk.

1.3 Standard Acknowledgements for Spitzer Publications

Any paper making use of the Spitzer scientific products should acknowledge the Spitzer project with the following text: “This work is based [in part] on observations made with the Spitzer Space Telescope, which was operated by the Jet Propulsion Laboratory, California Institute of Technology under a contract with NASA.” If you received NASA data analysis funding for the research, you should use one of the templates listed under http://irsa.ipac.caltech.edu/data/SPITZER/docs/spitzermission/publications/ackn/. Please see the Heritage Documentation Web site or the individual Spitzer Instrument Handbooks for further instructions of what acknowledgments to use when using data from specific instruments or observing programs.

Chapter 2. Spitzer History and Mission Overview

2.1 History and Organization of the Spitzer Project

The Spitzer Space Telescope began life as the Shuttle Infrared Telescope Facility (SIRTF) at the NASA Ames Research Center in 1971. The early history and subsequent development are described in detail by G. Rieke (2006, "The Last of the Great Observatories," Univ. Arizona Press) and by R. Rottner (2017, "Making the Invisible Visible", NASA SP-2017-4547). Key milestones in this history are:

June 1984: Selection of SIRTF instrument teams and Science Working Group.

1988: Decision to implement SIRTF in High Earth Orbit.

January 1990: Transfer of management responsibility for SIRTF from NASA Ames to JPL/Caltech.

1991: SIRTF selected as highest priority space astronomy mission for the 1990's by the decadal review panel chaired by John Bahcall.

Spring 1993: Selection of earth-trailing solar orbit for SIRTF.

November 1993: Adoption of warm launch architecture for SIRTF.

1995: Release of Request For Proposal (RFP) for selection of SIRTF contractors.

June 1996: Announcement of results of selection; formation of SIRTF project team.

August 1996: Designation of the Infrared Processing and Analysis Center (IPAC) at Caltech as the home of the SIRTF Science Center.

September 1997: Initiation of SIRTF Phase C/D – formal beginning of construction of SIRTF.

November 2000: Selection of the first SIRTF Legacy Science programs – large programs which established new modes of community participation in NASA missions.

August 25, 2003: Launch of SIRTF.

December 2003: Release of first SIRTF data and renaming of SIRTF as the Spitzer Space Telescope, to honor Lyman Spitzer, Jr.

September 2004: Publication of first Spitzer results in v.154 of the Astrophysical Journal Supplement.

May 2009: Depletion of Spitzer cryogen and end of the Cryogenic Mission.

July 2009: Start of Spitzer Warm Mission.

October 2016: Start of the Spitzer Beyond Mission.

January 29, 2020: Final observations executed

January 30, 2020: Decommissioning of the Spitzer Space Telescope, 6002 days since launch.

Although it took many years for Spitzer to go from Science Working Group/instrument selection to project start in 1996, the intervening years were not wasted; indeed, during this time the three instrument teams engaged in intensive detector technology development activities, resulting in an ensemble of focal plane arrays which achieved natural-background-limited performance even when used on a cryogenic space telescope. In the final realization, the teams used these arrays in ways which simplified instrument design and reliability. During this same time period, a very effective cryogenic optics development program led to a prototype all-beryllium telescope which was converted to the flight telescope after the selection of the contractor team.

The project organization for the development phase from 1996 to 2003 is shown in Figure 2.1. Ball Aerospace, which built the Cryogenic Telescope Assembly, including the telescope, cryogenic system, and associated shields and shells, was one of two major industrial partners. Ball also built the scan mirror mechanism for MIPS and was the contractor working with Cornell and U. Arizona to build the IRS and MIPS instruments, respectively. The other major industrial partner was Lockheed Martin Sunnyvale, which provided the spacecraft, the solar panel, and the system engineering, integration, and test for the observatory. NASA Goddard Space Flight Center was contracted by Harvard-SAO to build the IRAC instrument. The instrument Principal Investigators and their institutions are listed in Section 2.3 below. Spitzer had no foreign partners during the development phase, although scientists from across the world have applied successfully for observing time on Spitzer during the operations phase.

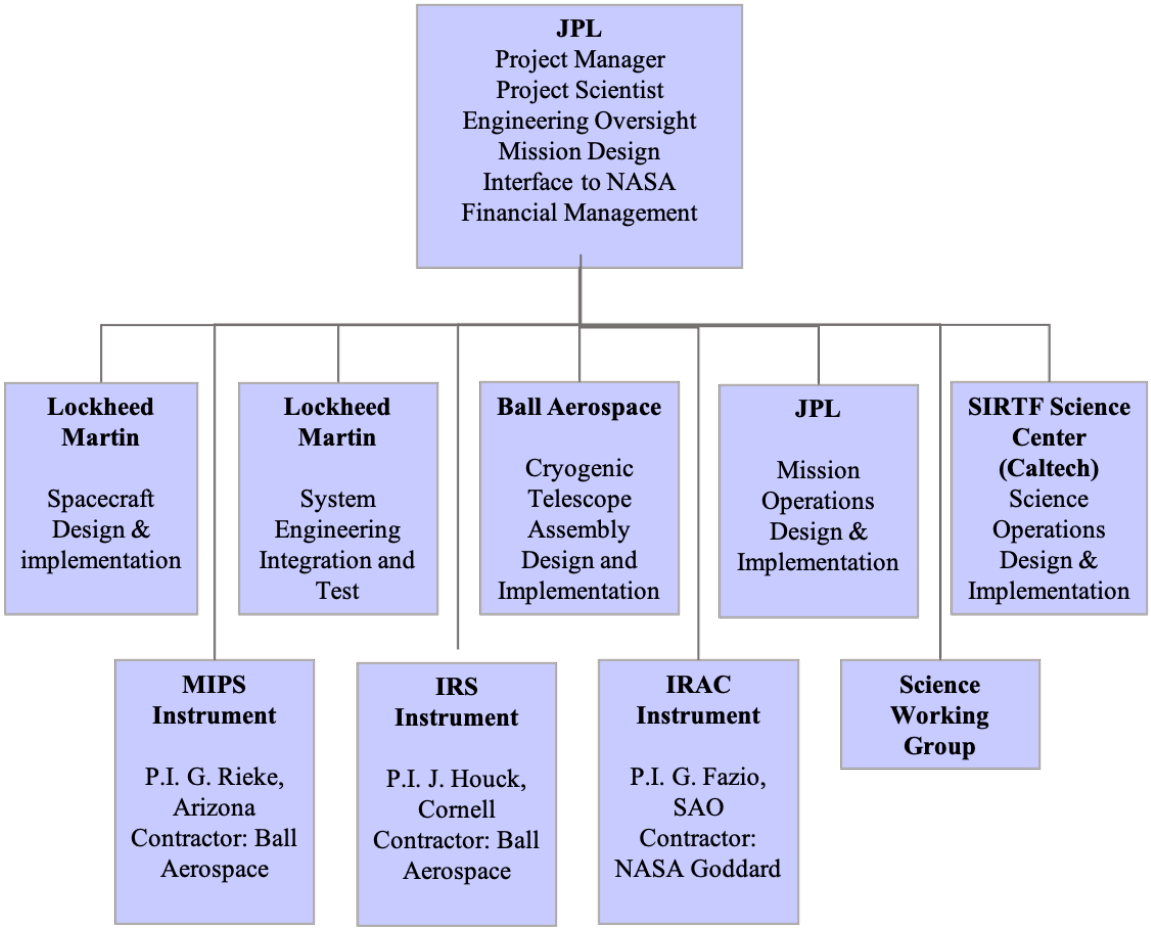

Figure 2.1: Spitzer Project organization during development phase 1996 - 2003. This diagram portrays functional responsibilities rather than reporting paths.

The launch of Spitzer was followed by two-month in-orbit checkout and one-month science verification phases which were paced by the cool down of the telescope. Execution of the Spitzer science program began on 1 December 2003, and the first public data release and naming of the observatory occurred later that month. During this time, the project organization was changed to one more appropriate for the operations phase of the mission, as is shown in Figure 2.2. In this transition, Lockheed Martin Sunnyvale was superseded by Lockheed Martin Denver, who took responsibility for spacecraft operations. Ball Aerospace monitored the performance of the cryogenic system and estimated the amount of helium remaining. Day-to-day responsibility for the science instruments was transferred, by pre-agreement, from the instrument teams to the Spitzer Science Center. The Ball Aerospace support ended with the depletion of the helium and the transition to the Spitzer warm mission. Also at this time, the operational responsibilities of the Spitzer Science Center for the IRS and MIPS instruments terminated since they were not used in the warm mission.

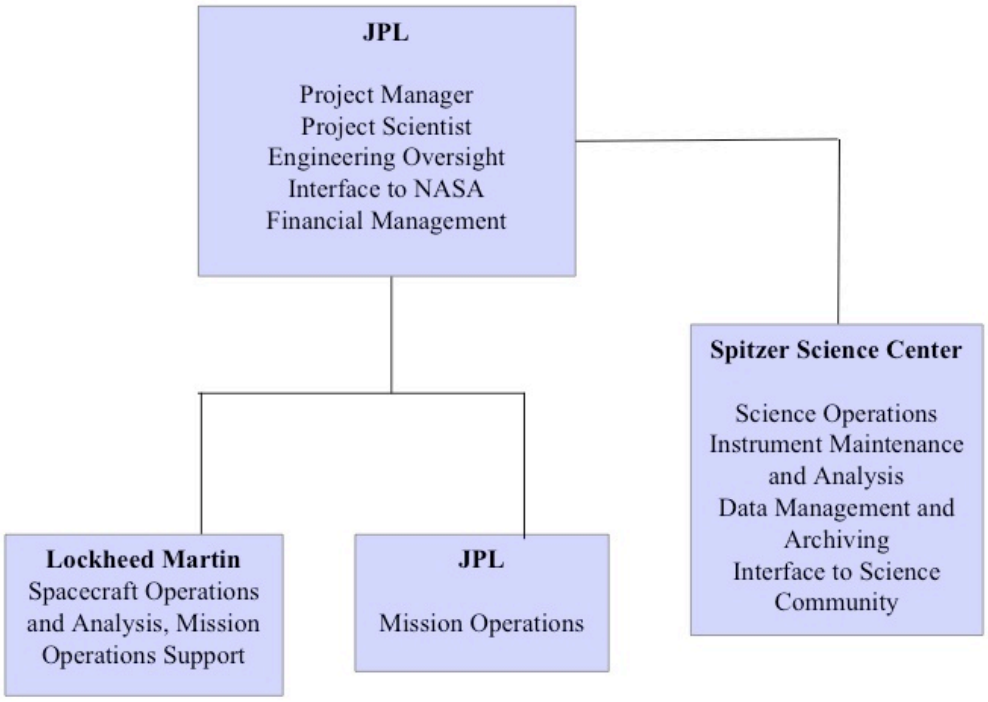

Figure 2.2: Spitzer Project organization during operations phase, 2003-2020. This diagram portrays functional responsibilities rather than reporting paths.

Spitzer was supported within NASA by the Astrophysics Division of what is now called the Science Mission Directorate. Programmatically, Spitzer completed NASA's family of Great Observatories, which also includes the Hubble Space Telescope, the Chandra X-Ray Observatory, and the Compton Gamma Ray Observatory (superseded by the Fermi Gamma Ray Telescope). Like its sister Great Observatories, Spitzer was operated as an observatory for the entire scientific community, with the bulk of the observing time (>80% during the cryogenic mission; 100% during the warm mission) available to the international scientific community through a peer-reviewed time allocation process.

A largely complete list of the many people who worked on the Spitzer project development and thus contributed to the great success of Spitzer is given in Werner et al. (2004) and updated at the end of this document in Appendix C. However, it is appropriate here to single out the six outstanding Project Managers who led the project during development and operations. These are: Larry Simmons who served from 1993 to 1999, David Gallagher (1999-2004), Robert Wilson (2004-2010), Suzanne Dodd (2010 - 2016), Lisa Storrie-Lombardi (2016-2019) and Joseph Hunt (2019-2021).

Overviews of the Spitzer mission during the cryogenic phase are given by M. Werner et al. (2004, ApJS, 154, 1) and by R. Gehrz et al. (2007, Rev. Sci. Inst., 78, 1302). The scientific bounty of Spitzer is described by M. Werner and P. Eisenhardt in "More Things in the Heavens: How Infrared Astronomy is Expanding our View of the Universe", published by Princeton University Press in 2019.

2.2 Spacecraft Development

The development of the flight system, apart from the instruments, was done by contractors Ball and Lockheed following a feasibility study of the warm launch architecture done at JPL. The instrument designs were done by the Principal Investigators working with their suppliers as described above. The Spitzer design is described in detail by R. Gehrz et al. (2007, Rev. Sci. Inst., 78, 1302) and M. Werner (2006, A&G, 47, 6.11); the design and implementation incorporates a number of innovations which may be summarized as follows:

2.2.1 A Prime Directive

The Spitzer telescope and its three science instruments were cooled to their ultimate operating temperatures by liquid helium cryogen, which itself achieved a temperature of about 1.2 K under the pumping action of the vacuum of space. The cooling was necessary to minimize the intrinsic infrared radiation of the telescope structure and to reach the optimum operating point for the detectors in the instruments. Approximately 350 liters of helium were loaded into the Spitzer cryogen tank (Figure 2.3) prior to launch, and when the last helium boiled away in May 2009, the primary Spitzer cryogenic mission ended. Thus the prime directive for the design of the Spitzer mission was to minimize the unnecessary, or parasitic, heat reaching the helium tank. This dictated both the choice of Spitzer's unusual orbit and the unusual architecture of Spitzer's cryogenic/thermal system.

The design of the cryogenic/thermal system isolated the telescope and instrument chamber so well that after the liquid helium was depleted they remained at temperatures cold enough to still use the shortest two channels on the IRAC camera. These two channels were used for over 10 years after the cryogenic mission ended during the warm mission.

2.2.2 A Kinder, Gentler Orbit

All previous space observatories had used a low Earth orbit (e.g., IRAS and the Hubble Space Telescope) or a high Earth orbit with a period of one-to-two days (e.g., ISO and the Chandra X-Ray Observatory). Spitzer broke this pattern by utilizing an Earth-trailing heliocentric, or solar orbit with semi-major axis very slightly larger than that of the Earth's orbit. As seen from Earth, Spitzer recedes at about 0.1 AU per year and reached a distance of 0.62 AU in five years. This orbit satisfies the Prime Directive in several ways. First, there is great benefit in getting away from the heat of the Earth. Second, the orbit allows radiative cooling into the refrigerator of deep space to play a large part in cooling Spitzer, and in keeping it cool. Third, because there are no eclipses, and the Earth and Moon are far away, the orbit permits excellent sky viewing and observing efficiency.

The orbit has one major disadvantage. As Spitzer moves away from the Earth, its radio signals become gradually weaker due to the increasing distance. The data is stored on board and radioed back to Earth through the dishes of the Deep Space Network (DSN). The nominal downlink strategy of one or two ~45 minute passes per day and a downlink data rate of 2.2 Mb/s worked for the cryogenic mission, although the largest DSN dishes (70 meters) were required for the final years of the cryogenic mission and until the spacecraft was decommissioned. During the warm mission Spitzer continued to drift further from the Earth, although this issue was partly mitigated by reduced data collection rates in this phase. At the time the spacecraft was decommissioned the downlink rate was 512 kB/s using either one 70-m or a combination of one 70-m and one 30-m

DSN dish. Downlinks were 120 to 150 minutes long and typically occurred 3 to 4 times a week, and the spacecraft was 1.77 AU from Earth.

2.2.3 Flight System Architecture

Spitzer's novel cryogenic architecture and the overall configuration of the flight system are shown in Figure 2.3. The spacecraft and solar panel were provided by Lockheed Martin. The telescope, instruments, cryostat, and associated shields and shells make up the Cryogenic Telescope Assembly (CTA), built by Ball Aerospace.

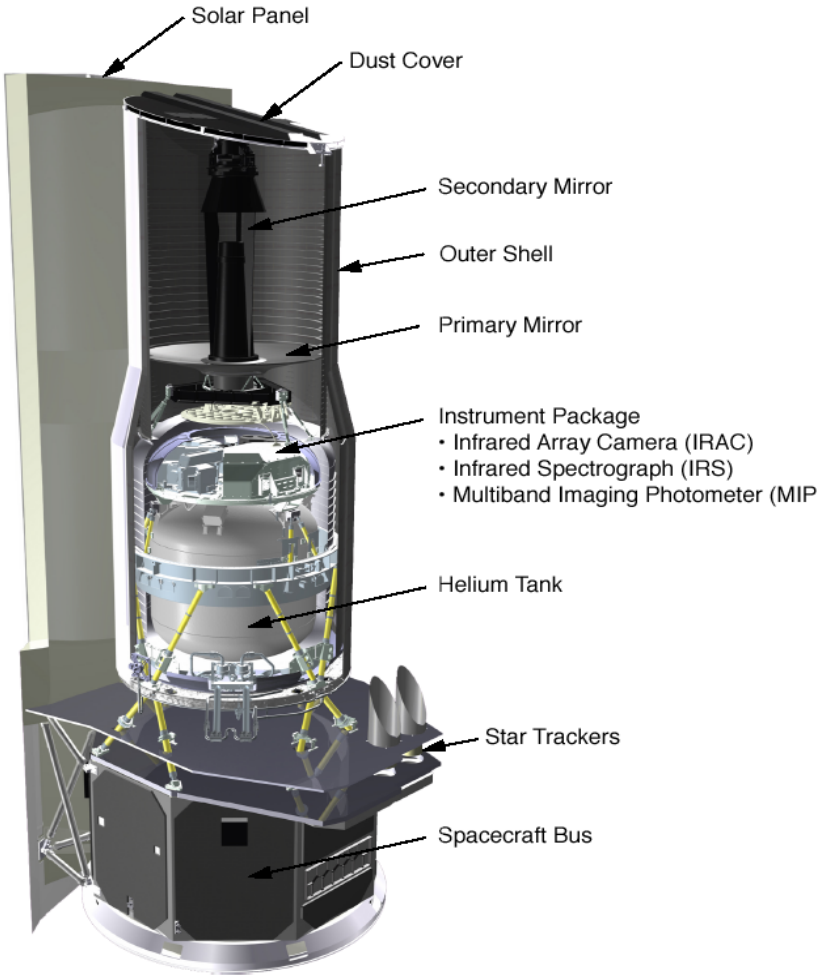

Figure 2.3: The outer shell forms the boundary of the CTA, which incorporates the telescope, the cryostat, the helium tank, and the three instruments. Principal Investigator-led teams provided the instruments, while Ball Aerospace provided the remainder of the CTA. Lockheed-Martin provided the solar panel and the spacecraft bus. The observatory is approximately 4.5m tall and 2.1m in diameter; the mass at launch was 861kg. The dust cover atop the CTA was jettisoned 5 days after launch. (Image courtesy of Ball Aerospace).

The novel features of the Spitzer cryo-thermal design and the benefits it bestows are illustrated in Figure 2.4, which compares the architecture of Spitzer as it now flies with an earlier design which resembles that of the predecessor ISO and IRAS missions. ISO and IRAS packaged the telescope inside the cryostat so that it was in close conductive contact with the liquid helium and thus cold at launch. Spitzer employed a novel design in which the greater part of the CTA was launched while at room temperature; only the science instrument cold assemblies and the superfluid helium vessel were cold within the vacuum cryostat shell. As shown in Figure 2.4, this allowed a much smaller vacuum pressure vessel and a smaller observatory mass than achieved by the cold launch architecture while maintaining telescope size and lifetime.

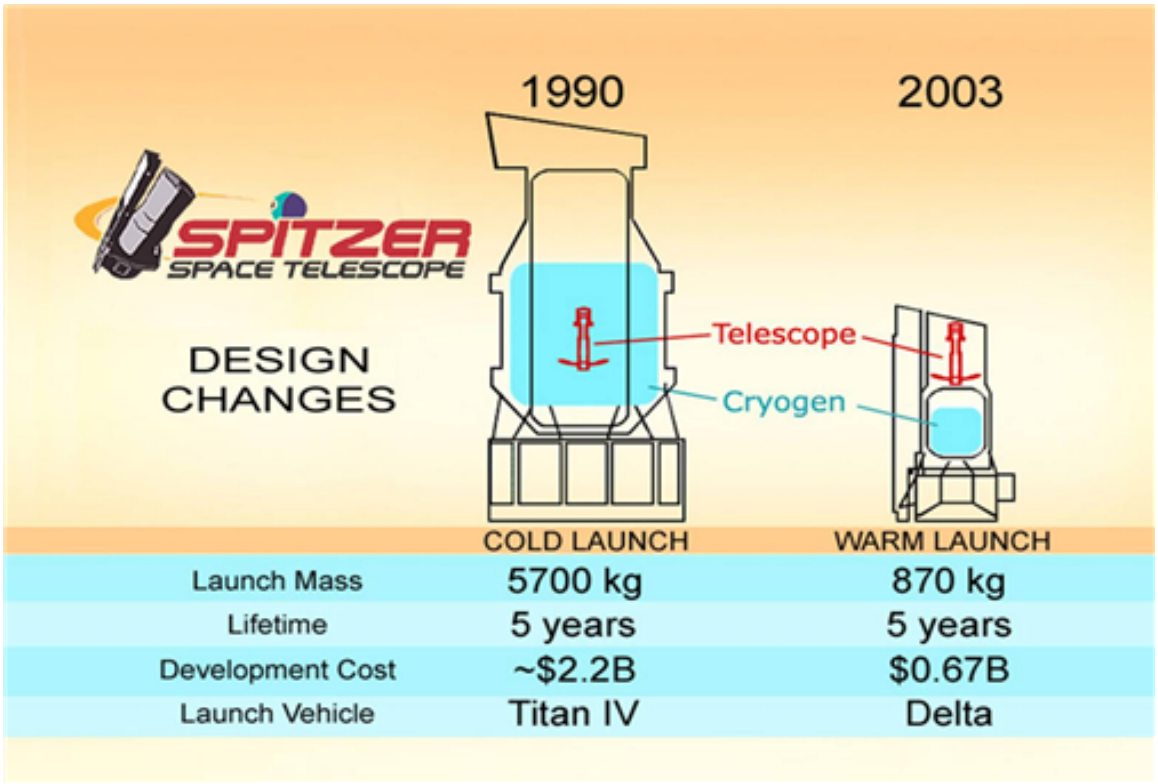

Figure 2.4: The warm launch architecture of Spitzer as it was flown [right] is compared with an earlier cold launch concept similar to the predecessor IRAS and ISO missions. The warm launch concept achieves the same mission lifetime and primary mirror size as the cold launch approach, but at a fraction of the cost. Some of the reduction in cost and mass was achieved by streamlining Spitzer's measurement capabilities, but the warm launch concept retains the core functionality required for the execution of Spitzer's most important programs.

For the longest wavelengths Spitzer required the telescope be at ~5.5K and the deep space refrigerator, together with the boil-off of the liquid helium, got us there after launch. The principles of this on-orbit cooling are deceptively simple. In the solar orbit, the spacecraft can be oriented so that the sun always falls on the solar panel, which shades the telescope outer shell. A carefully designed and fabricated system of reflective shells and shields assures that little of the solar heat reaches the outer shell to diffuse inward to heat the telescope. A similar system deflects heat from the spacecraft bus, which operates near room temperature. With no heat input, the telescope should cool very rapidly by radiating its heat to space – the anti-solar side of the

outer shell is painted black to facilitate this. Prior to launch it was predicted that the telescope would achieve a temperature below ~50K through this radiative cooling, and that the evaporating helium gas, which is at a temperature of only ~1.2K, would cool the telescope to its operating temperature of ~5.5K and keep it there.

The system worked just as predicted, if not better. The initial (radiative plus gas-assisted) cooldown to ~5.5 K took about 40 days. The outermost CTA shell equilibrated at an operating temperature of 34 to 34.5 K solely by radiative cooling, so that there is very little parasitic heat leaking inwards to the helium tank. It took only about one ounce of helium per day to keep Spitzer cold. Not coincidentally, this is about the same rate at which the instruments boiled away the liquid helium by dissipating power into the helium bath. So the system was both in equilibrium and in balance thermally.

2.2.4 The Spitzer Warm Mission

In May 2009, the last of Spitzer's helium boiled away. The cryogenic portion of the CTA started to warm up, but the passively-cooled outer shell stayed at a temperature near 35K. The telescope was cooler because it could radiate through the aperture at the top of the outer shell, and it equilibrated at 27.5 K. It was anticipated that the two shortest wavelength channels (channels 1 and 2) of the IRAC instrument at 3.6 and 4.5 microns would operate with full efficiency and sensitivity under these conditions, (although Spitzer's other channels would be inoperative), and plans were in place to continue to operate in what is now known as the Spitzer Warm Mission. During the Warm Mission the sensitivity and image quality were virtually unchanged from the cryogenic mission. Spitzer was operated as a facility for the entire astronomical community, with all of the observing time available to the user community through the usual peer-review process. The Warm Mission lasted from July 2009 until September of 2016.

In this document the phrase 'the warm mission' collectively refers to the Warm and Beyond Missions.

2.2.5 The Spitzer Beyond Mission

The Spitzer Beyond Mission lasted from October of 2016 until the telescope was decommissioned on January 30, 2020. Because of Spitzer's orbit and age, the Beyond phase presented a variety of new engineering challenges. Spitzer trails Earth in its journey around the sun, but because the spacecraft travels slower than Earth, the distance between Spitzer and Earth has widened over time (Figure 2.5). Spitzer communicated with Earth through an antenna fixed on the bottom of the spacecraft, so entire spacecraft had to be properly oriented to transmit and receive data. Early on, this could be done while keeping the sunlight incident on the solar panel within the original design limit of 30 degrees. In the Beyond Mission (Figure 2.5), the orbital geometry required that this incidence angle be as large as 55 degrees, so that the battery was used to help to power the downlinks, and had to be recharged during operations following the downlink session. At the same time, in these extreme orientations, sunlight was incident through the back of the spacecraft on structures which had been intended to be permanently shadowed, which might have impacted the system's pointing performance. Fortunately, these considerations had minimal impacts on Spitzer's scientific performance, and Spitzer returned excellent data right up to the end of the mission.

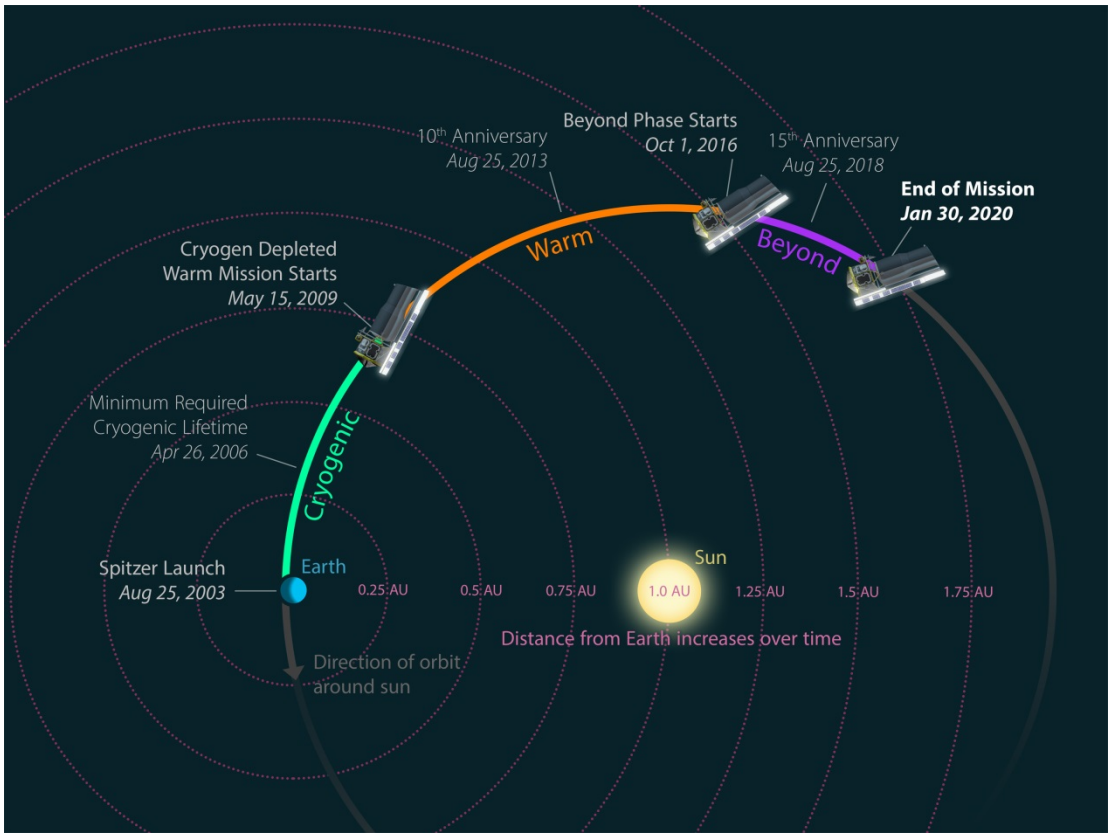

Figure 2.5: The phases of the Spitzer Mission from launch to decommissioning. In this diagram Spitzer is shown at the pitch angle needed to communicate with Earth. As the mission progressed, this angle increased. In this document the phrase 'the warm mission' collectively refers to the Warm and Beyond Missions

2.2.6 The Rest of the Story

Additional innovations as well as careful design, fabrication, and testing characterize the rest of the Spitzer spacecraft. Key components, described in detail in R. Gehrz et al. (2007, Rev. Sci. Inst., 78, 1302), include:

1. An all-Beryllium telescope, with an 85 cm primary mirror. Beryllium was selected because of its high strength-to-weight ratio and reproducible cryogenic behavior. The secondary mirror of the telescope could be moved in an axial direction to focus the telescope on-orbit. Pre-launch test and analysis determined the proper setting of the secondary. Only a small adjustment (less than .01 mm) in the position of the secondary was made after on-orbit cooldown to bring the telescope into proper focus. The telescope achieved diffraction-limited performance at all wavelengths longward of 5.5 microns across its entire focal plane, which had a radius of about 15 arcminutes. Spitzer achieved an image size of ~2 arcseconds at its shortest operating wavelengths.

2. *An excellent pointing and control system.* This system was built around a high performance autonomous star-tracker – which pointed the telescope to the desired star-field by using a pattern recognition algorithm based on an internal star catalog. In addition, the system included gyroscopes, reaction wheels to turn the spacecraft, and a visible light sensor in the telescope focal

plane to establish and track the line of sight of the cold telescope relative to that of the warm star tracker. The overall performance was excellent; Spitzer could be pointed to an accuracy of less than one-half arcsecond and achieved short-term stability much less than 0.1 arcseconds.

3. *A robust spacecraft.* The spacecraft bus shown in Figure 2.3 provided the Spitzer telescope and instruments with a robust and reliable support system. The spacecraft performed a variety of functions including pointing Spitzer; managing execution of the science program by clocking through a series of pre-loaded commands; storing, compressing and telemetering the science data to Earth; and monitoring its own health as well as that of the telescope and instruments. The Spitzer spacecraft resembles other unsung heroes in that when it operates smoothly (which it did essentially 100% of the time) we were unaware of its existence. After almost 16.5 years in orbit, the spacecraft remained fully redundant (it had two fully functional independent sides of electronics). The Spitzer spacecraft included one expendable substance, high-pressure nitrogen gas, used to spin down the reaction wheel assemblies when they start to accumulate too much angular momentum. At the time of decommissioning, enough nitrogen remained on board for Spitzer to control its attitude for several years.

4. *Detector Arrays.* The properties and power of Spitzer's detector arrays are well known to users of the observatory, and, by implication, to anyone who has seen some of Spitzer's spectacular images or spectra. The arrays and their applications in the Spitzer instruments are discussed in detail in subsequent sections of this documentation. Here we merely emphasize that Spitzer's great scientific power follows directly from the size and quality of the arrays used at all wavelengths and throughout the focal plane – both for imaging and spectroscopy. It is here that Spitzer achieved its gain over previous cryogenic observatories: IRAS flew single detectors, and ISO's few small arrays covered only a small fraction of its entire wavelength range. Spitzer as a cryogenic observatory in space achieved a thousand-fold increase in sensitivity at wavelengths beyond 3 microns over what could be done from within the atmosphere. When this increase in sensitivity is exploited by arrays with tens of thousands of pixels, the scientific grasp and the gain over alternative facilities are measured in factors of millions.

2.3 Principal Investigators, Science Team, and User Community

Initially, only six scientists were selected for the Science Working Group, three instrument PI's and three at-large members. These were:

Giovanni Fazio, Harvard-SAO, PI for the Infrared Array Camera (IRAC)
Jim Houck, Cornell, PI for the Infrared Spectrograph (IRS)
George Rieke, U. Arizona, PI for the Multiband Imaging Photometer for SIRTF (MIPS)
Michael Jura, UCLA, Interdisciplinary Scientist
Frank Low, U. Arizona, Facility Scientist
Ned Wright, UCLA, Interdisciplinary Scientist

In addition, these scientists were joined on the SWG by three ex-officio members:
Nancy Boggess, NASA-HQ, Program Scientist
Michael Werner, NASA-Ames, Project Scientist and SWG Chair
Fred Witteborn, NASA-Ames, Deputy Project Scientist

2.3.1 Evolution of the Spitzer Science Working Group

The SWG remained remarkably stable over the ~20 years between selection and launch. The only original member who left the group was Deputy Project Scientist Fred Witteborn, who did not make the move to JPL when the SIRTF project was relocated in 1989-1990. However, several new members were added to the group – both to supplement the existing group and fill additional needs. Thus at launch the SWG had expanded to 13, including the Project Scientist (Werner) and his new Deputy. The new members were:

Dale Cruikshank, NASA-Ames, Planetary Science Representative
Robert Gehrz, U. Minnesota, Outreach Coordinator
Charles Lawrence, JPL, Deputy Project Scientist
Marcia Rieke, U. Arizona, Community Affairs Coordinator
Tom Roellig, NASA-Ames, Facility Scientist
Tom Soifer, Caltech, Director of the Spitzer Science Center [ex-officio]

In addition, the NASA Program Scientist has remained an ex-officio member of the SWG. A number of excellent NASA scientists, and detailees, have held that position over the years, and the SIRTF/Spitzer project has benefitted from their participation and oversight. They include Nancy Boggess , Bill Danchi, Jay Frogel, Jonathan Gardner, Fred Gillett, Doug Hudgins, Bill Latter , Dave Leisawitz, Keith MacGregor, Kartik Sheth, Eric Smith, Guy Stringfellow, Glen Wahlgren and Kimberly Weaver.

Although the instrument PI's had a business and contractual relationship to the Project Office, the SWG as a group had only an advisory role. Formally, the SWG makes recommendations to the Project Scientist concerning scientific and technical matters, and the Project Scientist passes these on to the Project manager, or brings to the SWG questions raised by the Project Manager. In practice, the non-PI SWG members were well-integrated into the activities of the Project Office and often headed important project-wide tiger teams and integrated product teams. In addition, the SWG played an extremely important role in SIRTF advocacy. Finally, each member of the SWG was allocated observing time on Spitzer (see below) and was responsible for defining scientific programs, analyzing data and publishing the results.

2.3.2 Spitzer Scientific Utilization

Most of the observing time on Spitzer during the cryogenic mission (82.2%) (and all the time during the warm mission) was awarded to the international astronomical community through the usual peer-review process, which was managed by the Spitzer Science Center. Four somewhat distinct categories of observing time were identified in during the cryogenic mission:

Guaranteed Time was awarded to the PIs on behalf of their instrument teams and to the other members of the SWG. During the first 2.5 years of the cryogenic mission, each instrument team was granted 5% of the observing time, which was shared among the two-to-three dozen scientists who were affiliated with each of the instrument teams. The non-PI members of the SWG, including the Project Scientist and his Deputy, shared equally in another 5% of the time. Two and one-half years was singled out for this purpose because it was the Spitzer Level 1 lifetime requirement (considerably exceeded by the actual cryogenic lifetime). Following the first 2.5 years, the instrument team share continued at 5% while the non-PI allocation ceased.

Director's Discretionary Time amounted up to 5% of the observing time. It was awarded at the discretion of the SSC Director to facilitate observations of new or time-critical phenomena which cannot be deferred to the next annual proposal cycle. In the warm mission Director's Discretionary Time totaled 10% of the time observed (see the end of section 3.1 for more information).

Legacy Science Program is an innovation in community utilization that was pioneered by Spitzer. The intent was to assure that Spitzer addressed critical scientific problems while producing a coherent legacy in the form of uniform, high quality databases of broad scientific interest. This was done by inviting proposals for large programs and funding the selected teams both to produce scientific papers and to create higher order data products that go far beyond the standard data products produced by the Spitzer Science Center. In the first Legacy selection, announced in 2000, six projects were selected and awarded a total of 3160 hours of Spitzer time, with over 700 hours going to the largest program. These programs were largely completed during the first year of the Spitzer mission, and additional Legacy programs were selected and carried out annually for the next four years until the completion of the cryogenic mission. In total 8691.4 hours were allocated to 32 Legacy science programs. During the warm mission, the spirit of the Legacy Science program was carried on in the Exploration Science and Frontier Legacy programs.

General Observer (GO) projects. All observing time on Spitzer not allocated into one of the previous three categories was awarded to General Observer projects, which cover a very wide range of scientific topics. These can include joint projects with other NASA observatories. The GO program continues during the Warm and Beyond Mission, utilizing all observing time (except the 10% Director's Discretionary Time).

In addition to these observational programs, Spitzer also had grants for theoretical research and programs doing archival research during the cryogenic mission. During both the cryogenic and warm missions, Spitzer offered joint time with observatories in some cycles, including the Hubble Space Telescope, Chandra X-Ray Observatory, NRAO and NOAO.

In aggregate 747 scientists from 38 countries were selected as Principal Investigators on Spitzer programs over the 5.7 years of the Spitzer cryogenic mission. During the warm mission 335 scientists from 22 countries were selected as Principal Investigators.

During the warm mission there were five categories of observations. In addition to the General Observer (GO) and Director's Discretionary Time (DDT) programs, three new program types were introduced:

Exploration Science Programs: The Exploration Science programs were science that required more than 500 hours of Spitzer observing time. Exploration Science programs provided an opportunity for large-scale investigations not practical during the cryogenic mission. In total 38,412.4 hours of Exploration Science in 42 programs were selected. The largest Exploration Science program selected was allocated 2108 hours.

Frontier Legacy Programs: Frontier Legacy programs were introduced in Cycle-13. The Spitzer mission began with Legacy programs - large, coherent science investigations that would provide a lasting legacy for the Spitzer mission in addition to the primary science goals of the program. The Frontier Legacy category was introduced to solicit programs that require substantially more time than the typical Exploration Science programs (which were introduced in Cycle-6). These programs were designed to create an important component of the legacy of the Spitzer mission. In

total there were three Frontier Legacy programs with allocations totaling 8545.1 hours, the largest single program was allocated 5286 hours.

Snapshot Programs: As the warm mission progressed the downlink rate dropped and the program complexity increased as more exoplanet and time series observations were approved. It became necessary to encourage programs to fill the gaps between these heavily constrained observations. Snapshot programs were designed to provide a substantial number of hours of easy to schedule, lower data volume science and were selected with the understanding that only a sampling of the proposed sources might be observed.

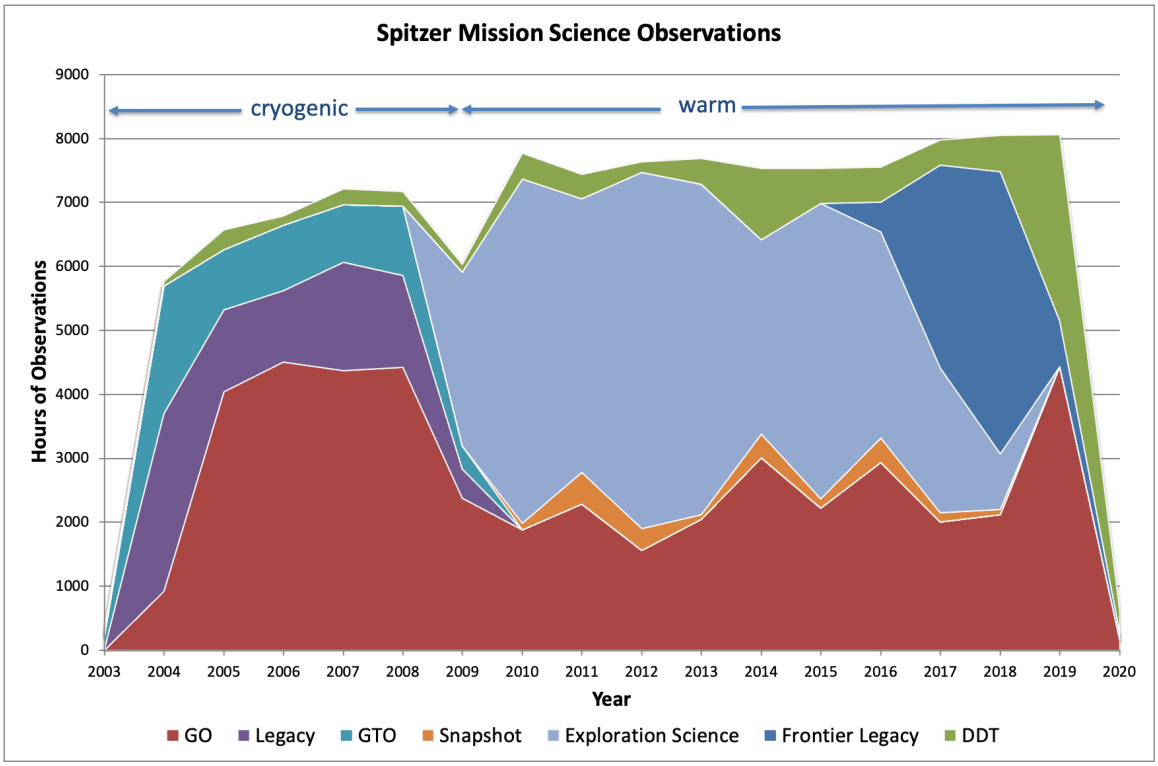

Figure 2.6: Program types for science observations in the Spitzer mission. The cryogenic mission ran from August 2003 to May 2009, and the warm mission ran from July 2009 to Jan 2020. Legacy and GTO programs were cryogenic mission only, Exploration Science, Frontier Legacy and Snapshot programs were warm mission only. The dip in hours of observations during 2009 is due to IWIC. DDT time increased in 2014 for the Frontier Fields, and at the end of mission (see section 3.1)

Chapter 3. Observatory Description

The information in the next two chapters is gleaned from the Spitzer Observer's Manual, the primary source of technical information for planning Spitzer observations during the mission.

3.1 Overview

Spitzer was launched from Cape Canaveral, Florida into an Earth-trailing heliocentric orbit on 25 August 2003. The observatory was launched with the telescope at ambient temperature; only the focal plane instruments were cooled to cryogenic temperatures. The telescope gradually cooled to ~30 K over a period of ~45 days. Liquid helium was used to further cool the telescope to 5K.

Following launch, Spitzer entered a 63-day In-Orbit Checkout (IOC) phase, followed by a 35-day Science Verification (SV) phase, during which the planned capabilities of the telescope were verified, the detailed performance characterized, and the three science instruments and their operational modes commissioned. Following the completion of IOC/SV, Spitzer was commissioned for routine cryogenic science operations on 1 December 2003. Only one science instrument could be on at any given time so observations were done in instrument campaigns ranging from ~ 7 – 21 days in length. The order of the campaigns during the cryogenic mission was IRAC – MIPS – IRS. This order permitted the optimal cryogen usage by matching telescope temperature to the needs of the instrument in use, as discussed in Werner, M. (2012, SPIE, 51, 011008).

The cryogenic mission continued until the exhaustion of the onboard cryogen used to cool the telescope and science instruments. The Spitzer cryogenic lifetime requirement was 2.5 years of normal operations, which was passed on 26 April 2006. Due to the excellent performance of the cryogenic system after launch, the utilization strategy described above, and the implementation of warm and cold MIPS campaigns begun at the start of Cycle-3 (August 2006) to further extend the prime mission the actual cryogenic lifetime was ~5.5 years. The cryogen was depleted on 15 May 2009.

The first science observations during the prime mission included the First Look Survey (FLS), which was conducted by the SSC on behalf of the Spitzer observer community. The FLS was a ~110-hour survey using Director's Discretionary Time. The goals of the FLS were to provide a characteristic first look at the mid-infrared sky at Spitzer sensitivity levels and to rapidly process the data and place it in the public domain in time to impact early Spitzer investigations (specifically, Cycle-1 planning). The first science also included Guaranteed Time Observer (GTO) and Legacy Science observations. About 6 months after IOC/SV was completed Cycle-1 General Observer (GO) observing commenced (June 2004). The majority of the original Legacy Science observations (the data of which were made public immediately) were completed within the first 18 months of the prime mission. In Cycles 2 and up, GO, GTO, DDT and Legacy Science were executed concurrently.

The Spitzer Science Archive opened in May 2004, and initially contained FLS data, early release observations, and any Legacy data taken and reprocessed with the most current pipelines at that time. The start and end dates for each cycle of proposals were:

Cryogenic Mission

- Original GTO and Legacy Science: Dec 1, 2003 - April 2006
- Cycle-1: July 2004 - May 2005
- Cycle-2: June 2005 - May 2006
- Cycle-3: June 2006 - June 2007
- Cycle-4: July 2007 - June 2008
- Cycle-5: July 2008 – May 15, 2009

Warm and Beyond Missions

- IRAC Warm Instrument Characterization (IWIC): May - July 2009
- Cycle 6 Exploration Science: Aug 2009 - Aug 2011
- Cycle 6 GO: Aug 2009 - July 2010
- Cycle 7: Aug 2010 - July 2011
- Cycle 8: Aug 2011 - Dec 2012
- Cycle 9: Nov 2012 - Dec 2
- Cycle 10: Dec 2013 - Feb 2015
- Cycle 11 Exploration Science and Large Programs: Feb 2015 - Sep 2016
- Cycle 11 GO: Feb 2015 - Dec 2015
- Cycle 12: Dec 2015 - Sep 2016
- Cycle 13: Oct 2016 - Oct 2018
- Cycle 14: Nov 2018 - Jan 29, 2020

During the 2016 NASA Senior Review process, the agency made a decision to close out the mission in 2018 in anticipation of the launch of the James Webb Space Telescope, which will also conduct infrared science. Since Cycle 13 was planned to be a two-year cycle, two smaller DDT proposal calls occurred in February and September of 2017 to provide opportunities for science that could not be proposed in Cycle 13. When Webb's launch was postponed, the Spitzer mission was granted its fifth and final extension until January of 2020. Cycle 14 was selected to fill this time, with two more DDT proposal calls in March and May of 2019. DDT proposals continued to be accepted on an ad hoc basis until the end of 2019.

3.2 Observatory Description

Spitzer is a 3-axis stabilized pointing and scanning observatory. The top-level observatory characteristics are summarized in Table 3.1. Spitzer's science payload consisted of three cryogenically-cooled instruments, which together offer observational capabilities stretching from the near- to the far-infrared.

Table 3.1: Summary of Spitzer Characteristics.

Aperture (diameter)	85 cm
Orbit	Solar (Earth-trailing)
Cryogenic Lifetime	5.5 years (est.); 5.7 years actual
Wavelength Coverage (passband centers)	3.6 - 160 μm (imaging) 5.3 - 40 μm (spectroscopy) 55 - 95 μm (spectral energy distribution)
Diffraction Limit	5.5 μm

Image Size	1.5'' at 6.5 μm
Pointing Stability (1σ, 200s, when using star tracker)	<0.1''
As commanded pointing accuracy (1σ radial)	<0.5''
Pointing reconstruction (required)	<1.0''
Field of View (of imaging arrays)	~ 5'x5' (each band) except for: 70 μm: 2.5'x5' 160 μm: 0.53' x 5.33'
Telescope Minimum Temperature	5.6 K (cryo); 27.5 K (warm)
Maximum Tracking Rate	1.0''/ sec
Time to slew over ~90º	~8 minutes

The InfraRed Array Camera (IRAC) – Giovanni G. Fazio, Smithsonian Astrophysical Observatory/Harvard-Smithsonian Center for Astrophysics, PI

IRAC provided images at 3.6, 4.5, 5.8 and 8.0 microns, with two adjacent 5.2' x 5.2' fields of view. One field of view images simultaneously at 3.6 and 5.8 microns and the other at 4.5 and 8.0 microns via dichroic beamsplitters. All four detector arrays are 256 x 256 pixels with 1.2 arcsecond square pixels. During the warm mission, only the 3.6 and 4.5 micron arrays remained operational.

The InfraRed Spectrograph (IRS) – James R. Houck, Cornell University, PI

IRS performed both low and high-resolution spectroscopy. Low-resolution, long slit spectra ($\lambda/\Delta\lambda$ = 64–128) could be obtained from 5.2 to 38.0 microns. High-resolution spectra ($\lambda/\Delta\lambda$ ~600) in Echelle mode could be obtained from 9.9 to 37.2 microns. The spectrograph consists of four modules, each of which is built around a 128×128 pixel array. One of the modules incorporated two peak-up windows that could be used in locating and positioning sources on any of the four spectrometer slits with sub-arcsecond precision. Each IRS Peak-Up window has 1.8 arcsecond square pixels and a field of view of 1' x 1.2'. One of the windows covered 13.5–18.5 microns (blue) and the other 18.5–26 microns (red). Due to the higher operating temperatures IRS was not operational during the warm mission.

The Multiband Imaging Photometer for Spitzer (MIPS) – George H. Rieke, University of Arizona, PI

MIPS was designed to provide photometry and super resolution imaging, as well as efficient mapping capabilities, in three wavelength bands centered near 24, 70 and 160 microns. The array materials, sizes and pixel scales vary; they are given in Table 3.2. MIPS was also capable of low-resolution spectroscopy ($\lambda/\Delta\lambda$ ~15–25) over the wavelength range 55–95 microns and a Total Power Mode for measuring absolute sky brightness. Due to the higher operating temperatures MIPS was not operational during the warm mission.

Table 3.2: Spitzer Instrumentation Summary (NB: limits include confusion).

	λ (microns)	Array Type	λ/Δλ	Field of View	Pixel Size (arcsec)	Sensitivity (μJy) (5σ in 500 sec, incl. confusion)
IRAC	3.6	InSb	4.7	5.21'x5.21'	1.2	1.6 (3.4) / 2.3 (3.8)
	4.5	InSb	4.4	5.18'x5.18'	1.2	3.1 (4.3) / 3.2 (4.4)
	5.8	Si:As(IBC)	4.0	5.21'x5.21'	1.2	20.8 (21)
	8.0	Si:As(IBC)	2.8	5.21'x5.21'	1.2	26.9 (27)
IRS	5.2–14.7	Si:As(IBC)	64–128	3.7''x57''	1.8	250
	13.5–18.5 18.5–26	Si:As(IBC) Peak-Up	~3	54''x80''	1.8	116 80
	9.9–19.5	Si:As(IBC)	~600	4.7''x11.3''	2.3	1.2×10^{-18} W/m^2
	14.3–35.1	Si:Sb(IBC)	64–128	10.6''x168''	5.1	1500
	18.9–37.0	Si:Sb(IBC)	~600	11.1''x22.3''	4.5	2×10^{-18} W/m^2
MIPS	24	Si:As(IBC)	5	5.4'x5.4'	2.55	110
	70	Ge:Ga	4	2.7'x1.4' 5.2'x2.6'	5.20 9.98	14.4 mJy 7.2 mJy
	55-95	Ge:Ga	15–25	0.32'x3.8'	10.1	57, 100, 307 mJy (@60, 70, 90 μm)
	160	Ge:Ga (Stressed)	5	0.53'x5.33'	16×18	29 (40) mJy

Notes for Table 3.2: The sensitivities given are for point sources, and are only representative; IRAC sensitivity is given for intermediate background – the first number in each case without confusion, and the second number (in parentheses) includes confusion. For IRAC the numbers before the slash ("/") sign are for the cryogenic mission and the numbers after the slash sign are for the warm mission. IRS sensitivity is given for low background at high ecliptic latitude (note that for IRS, sensitivity is a strong function of wavelength); MIPS sensitivity is given for low background; 70 micron observations can be confusion limited; Because of a bad readout at one end of the slit, spectral coverage for 4 columns in MIPS SED is reduced to about 65-95 microns; 160 microns is often confusion limited, 29 mJy refers to no confusion and 40mJy refers to the estimated confusion limit.

3.3 Science Instrument Operations

Spitzer's payload was capable, but simple. Among the three science instruments there were only two moving parts: the shutter on IRAC (which was not used until the final days of the mission) and the scan mirror on MIPS. The observatory schedule was organized into instrument campaigns. Only one of the three instruments could be powered on at any one time, but all of the apertures (or observing modes) of that instrument were available whenever the instrument was on (with the exception that only one of the four IRS modules could be read out at a time). As shown in Figure 3.1, the apertures pointed toward different portions of the sky at the same time; switching apertures and staying on the same target in general required re-pointing the telescope. A few things to notice are that the IRS slits covered a wide range of orientations and that the MIPS fields of view were larger than the array size; this is because they show the range covered by the motion of the MIPS scan mirror.

A central concept in Spitzer science operations was that of the Astronomical Observation Templates (AOTs). The three science instruments are operated in nine discrete observing modes that offer the observer a selected number of choices in configuring and operating the instrument. These observing modes are known as AOTs. The AOT concept and the nine Spitzer AOTs are described in Chapter 4, and in greater detail in the Instrument Handbooks.

The SSC planned and executed calibration activities to maintain the instrument calibration. The instrument calibration for each instrument is discussed in the relevant Instrument Handbook. Information about cross-calibration is discussed in Chapter 5.

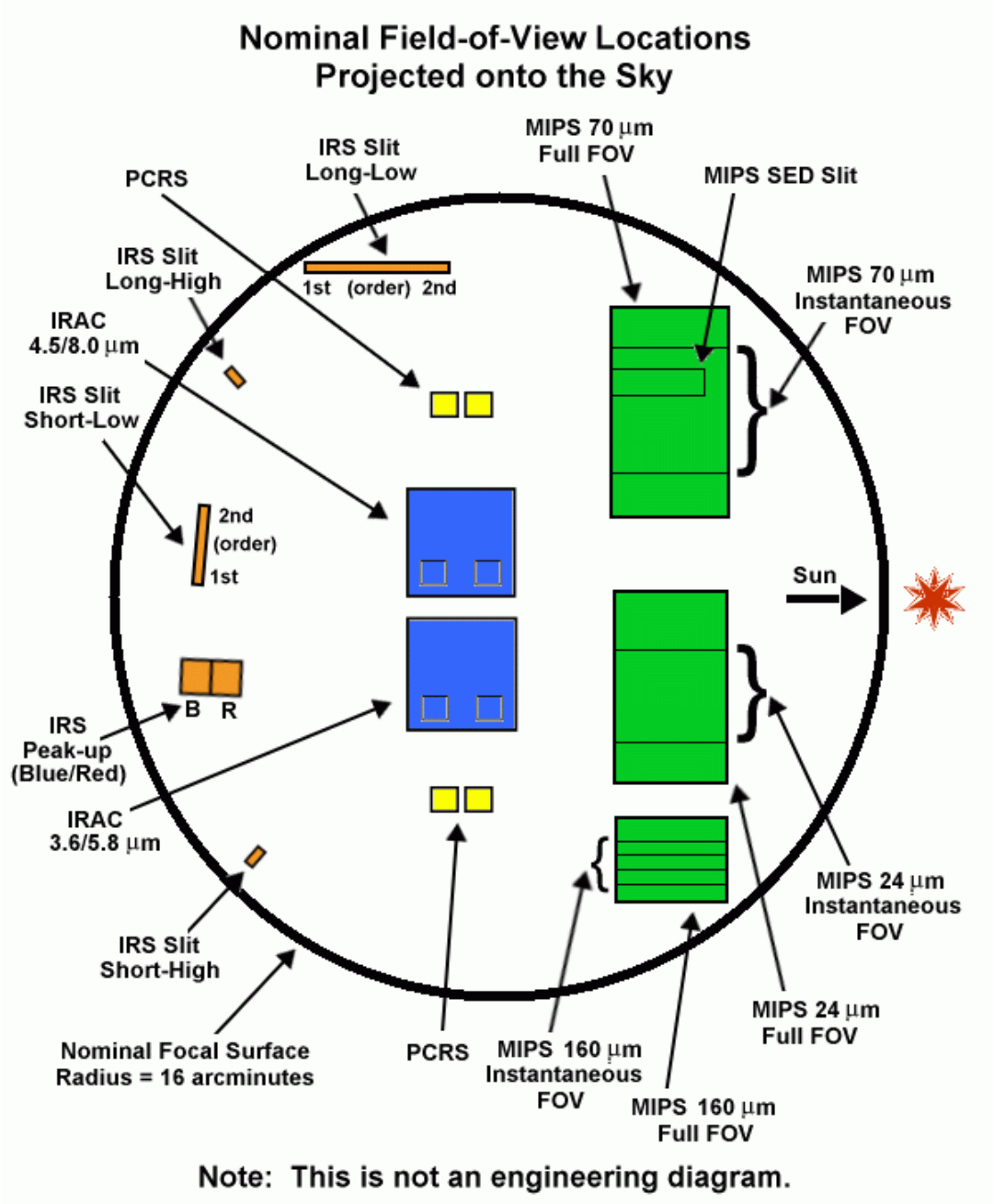

Figure 3.1: Science instrument apertures projected onto the sky. Because of the optical inversion in this projection, the section of sky closest to the projected Sun is on the MIPS side of the focal plane, e.g. to the right in this view. Because the spacecraft did not rotate about the line of sight, this vector is fixed relative to the focal plane on the sky. The IRAC sub-array fields are shown by the small boxes in the lower corners of both IRAC arrays. (The 8.0 and 5.8 μm sub-arrays are on the right and the 4.5 and 3.6 μm sub-arrays are on the left.) Note that for figure clarity, the widths of the IRS slits as shown are rendered substantially larger than their actual scale. The PCRS, or Pointing Control Reference Sensor, is a small visible wavelength array used initially to monitor the boresight alignment

of the telescope and the spacecraft star sensors and, subsequently, to position targets on spectroscopy slits and photometry arrays.

3.4 Observatory Design and Operations Concept

Spitzer is unique in many ways; the cryostat and mission design allowed a very long cryogenic lifetime (5.7 years) with a relatively small amount of cryogen (~360 liters of superfluid helium). [For comparison, IRAS had a 10-month lifetime using 560 liters of liquid helium, and ISO had a 28-month lifetime using 2140 liters of cryogen. During the prime mission the helium bath temperature was maintained at 1.24 K, the telescope temperature could be ≤ 6 K, and the outer shell temperature is approximately 34 K. Some of Spitzer's unique features were its Earth-trailing solar orbit and the fact that the telescope was launched at ambient temperature. This "warm launch" architecture and earth trailing helocentric orbit (which separated the telescope from the heat of the Earth) allowed Spitzer to achieve its lifetime goal with a smaller, lighter cryostat than would otherwise be required.

A basic external view of Spitzer is shown in Figure 3.2. The spacecraft provided structural support, pointing control, part of the instrument electronics, and telecommunications and command/data handling for the entire observatory. The spacecraft, including the spacecraft bus, the solar panel and Pointing and Control System (including the Pointing Control Reference Sensors, or PCRSs, which are located in the focal plane) were provided by Lockheed Martin Space Systems Company.

The CTA, shown in Figure 3.3, consists of the telescope, the superfluid helium cryostat, the outer shell group and the Multi-Instrument Chamber (MIC), which hosts the cold portions of the IRAC, IRS, and MIPS science instruments and the PCRS. The telescope assembly, including the primary and secondary mirrors, metering tower, mounting bulkhead (all made of beryllium) and the focus mechanism, was mounted and thermally connected to the cryostat vacuum shell. The barrel baffle of the telescope assembly was separately attached to the vacuum shell at its flange. The MIC, an aluminum enclosure containing the instrument cold assemblies, was mounted on top of the helium tank. The vapor-cooled shields, the vacuum shell and the outer shields are connected to the cryostat by a series of low connectivity struts. The CTA was provided by Ball Aerospace and Technologies Corporation.

The spacecraft and CTA (and science instruments) together comprise the observatory, which is ~4 m tall, ~2 m in diameter, and has a mass of ~900 kg.

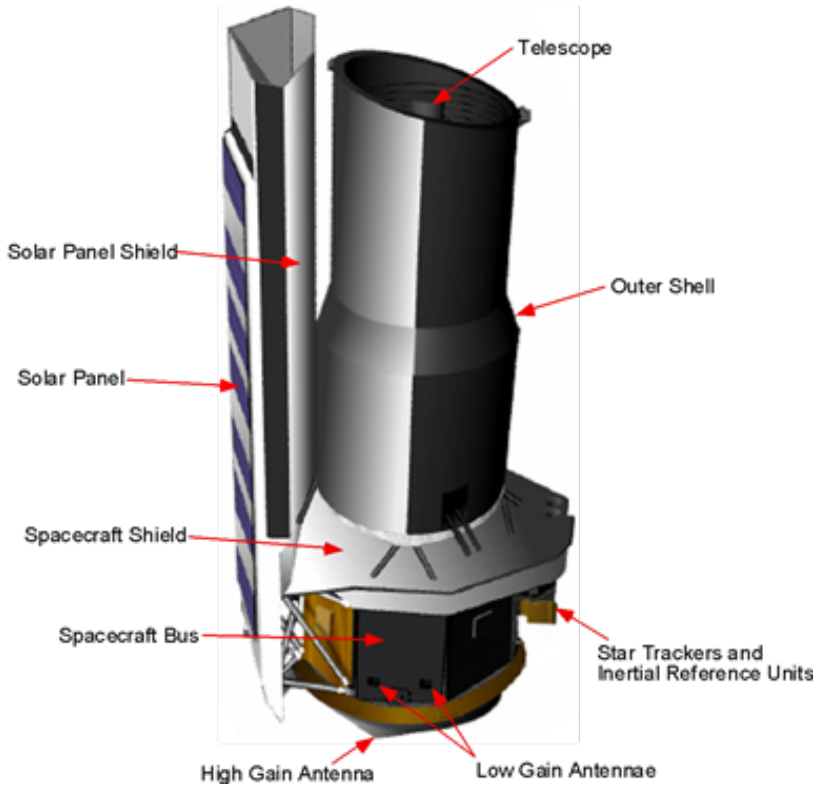

Figure 3.2: Basic external view of Spitzer. The observatory coordinate system XYZ (shown in Figure 3.4) is an orthogonal right-hand body-fixed frame of reference. The X-axis passes through the geometric center of the top surface of the spacecraft, is parallel to the CTA optical axis (which passes through the primary and secondary mirror vertices), and is positive looking out of the telescope. The Z-axis intersects the line forming the apex of the two surfaces of the solar panel. The Y-axis completes the right hand orthogonal frame. The X-axis origin is defined such that the on-axis point between the CTA support truss and the spacecraft bus mounting surface is located at X = +200 cm, in order to maintain positive X values throughout the observatory. The Sun always lies within 2º of the XZ plane (i.e., the roll angle is constrained to ±2º).

Spitzer executed autonomously a pre-planned, typically week-long, schedule of science observations, calibrations and routine engineering activities, which had been uploaded in advance and stored on board. During the cryogenic mission this "master sequence" might have up to 14 different 12–24 hour Periods of Autonomous Operation (PAOs), containing observations and calibration activities, each followed by a 30-60 minute period spent re-orienting the spacecraft for downlink and transmitting the data to the ground. IRS campaigns routinely had a 24-hour PAO with one downlink lasting longer than 40 minutes. At the end of the mission the data volumes were lower and a master sequence typically had 3-5 PAOs of 24-72 hours each and 3-4 downlinks to Earth of 120-150 minutes each. After the downlinks, Spitzer returned to the pre-planned sequence of observations and calibrations. Because efficient communication with the ground requires use of the high-gain antenna mounted on the bottom of the spacecraft (Figure 3.2), executing a downlink of the collected data required slewing the spacecraft to orient the high gain antenna toward one of the Deep Space Network (DSN) stations on Earth. Any of the three DSN sites (Canberra, Madrid and Goldstone) could be used when visible. During the time that data

were being transmitted to the ground, no science data could be collected. In extreme circumstances, Spitzer was designed to survive for up to a week with no ground contact at all.

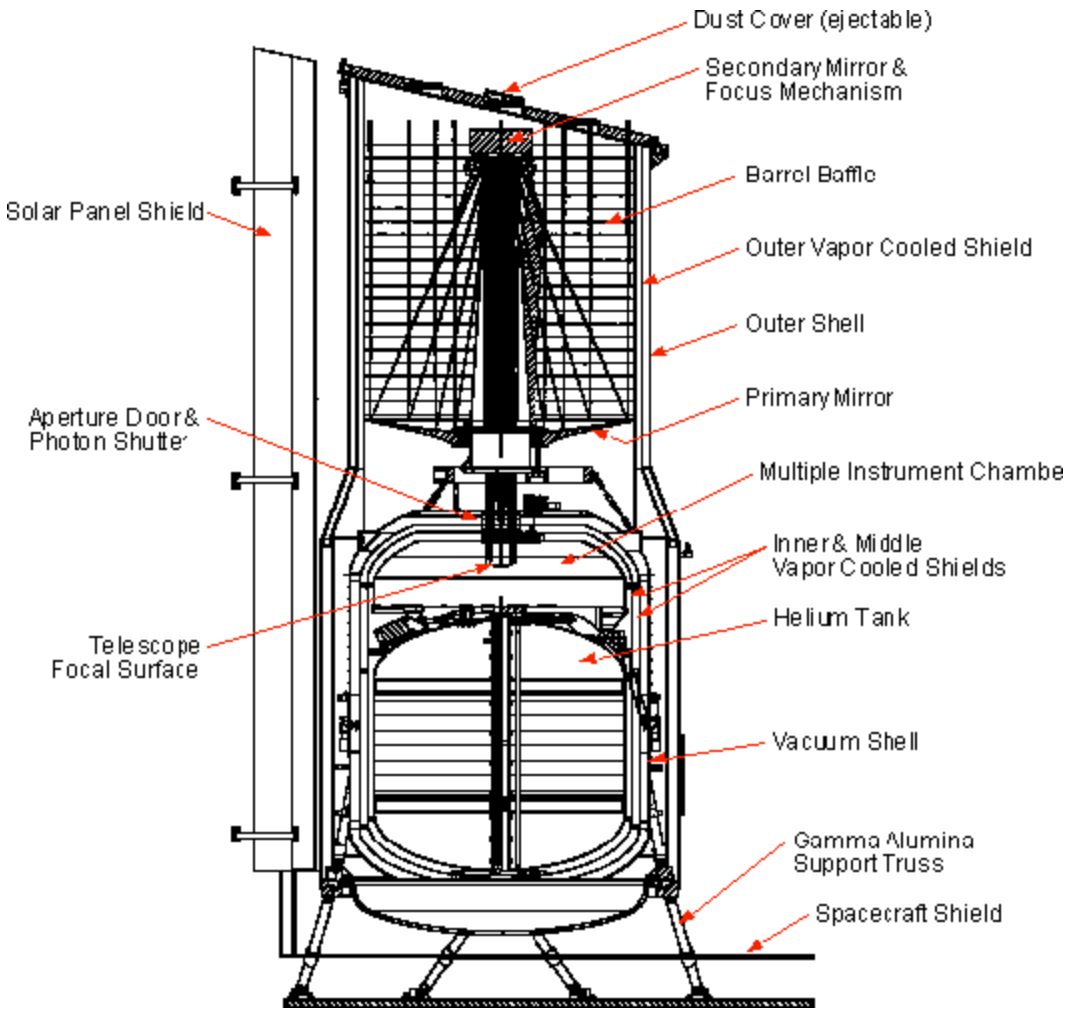

Figure 3.3: Cryogenic Telescope Assembly.

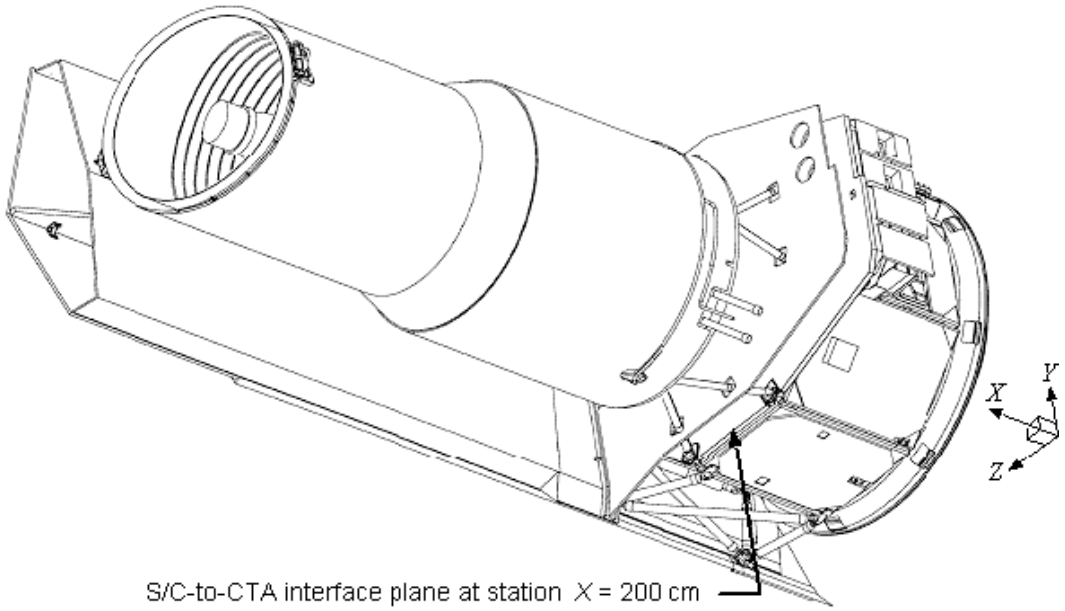

Figure 3.4: Observatory Coordinate System.

3.4.1 The Warm Launch and Telescope Temperature Management

One of the unique aspects of Spitzer is the warm launch concept. The telescope was at ambient temperature at the time of launch and gradually reached its lowest operating temperature (≤ 6K) approximately 45 days after launch, through passive cooling and by vapor vented from the cryostat. The science instruments were in contact with the helium bath at all times and were thus cold at the time of launch. The on-orbit performance confirms the soundness of the Spitzer thermal design principles.

Because the telescope was cooled by vapor vented from the cryostat, the telescope temperature depends upon how much power is dissipated in the cryostat. Because the cryogenic design and performance result in near-zero parasitic heat loads into the cryostat, the power entering the helium bath was essentially that of the instrument in use. Due to variations in the power dissipation of the instruments, the telescope temperature would naturally vary from ≤ 6 K to ~12 K. A "make-up" heater was available to add additional heat when needed to lower the telescope temperature. Since very low background is required for 160 μm observations, make-up heater operations were always planned to cool the telescope to ≤ 6 K and maintain it at that temperature during MIPS campaigns that are obtaining 160 microns observations. This is accomplished using a heat pulse that has been optimized to use the least amount of cryogen, while still guaranteeing a cold telescope for MIPS; it uses considerably less cryogen than holding the temperature constant all the time. The heat pulse is typically ~10 hours in duration and takes place about 10 days prior to the start of the MIPS campaign. The details of pulse size and duration were optimized to minimize cryogen usage and maximize scheduling efficiency.

In order to maximize Spitzer's cryogenic lifetime, starting in Cycle 2, MIPS campaigns were organized into "warm" (telescope cooled to ~8.5 K) or "cold" (~5.5 K) campaigns. AORs requiring 160 microns were scheduled only in cold (~5.5 K) MIPS campaigns. MIPS observations not requiring 160 microns were scheduled in warm (~8.5 K) or cold (~5.5 K) campaigns.

In the warm mission, both IRAC arrays were actively thermally controlled to 28.7K. The programmable voltages for each array were optimized. In addition to the operating temperature, the primary difference in array operation was a lower applied bias of 500 mV for the 3.6 micron array compared to 750 mV of applied bias in the cryogenic mission.

3.4.2 Data Storage

The Spitzer spacecraft includes the command and data handling subsystem (C&DH) which shares the flight computer (a RAD 6000) with the pointing control subsystem (PCS). The C&DH validates and executes either previously stored or real time commands, receives and compresses data, and writes the compressed data into the mass memory. The C&DH also provides a stable clock to correlate data and events.

During normal science operations, the observatory collects, compresses, and stores 12 to 72 hours' worth of science data prior to downlinking it. Spitzer has 16 Gbits of solid state memory (for both science and engineering data). During each 12 to 72-hour PAO, up to 6 Gbits of the memory are filled. Enough additional storage capacity is left unused during that 12 to 24-hour PAO to permit missing a downlink opportunity (e.g., due to a problem at the ground station) and continuing to observe without overwriting previously collected science data. Since the full mass memory (16 Gbits) is available to whichever of the two redundant flight computers is in use, in general multiple passes would have to be missed before the risk of losing science data that had not been transmitted to the ground becomes significant. However, e.g., MIPS sometimes generated enough data that a single missed pass could become important. During the warm mission the downlink rate decreased as the distance to the spacecraft increased, and data volume management became a driving force behind the scheduling process.

3.4.3 Data Transmission

Spitzer had two antenna systems for data uplink and downlink. The high gain antenna (HGA) supported a maximum downlink rate of 2.2 Mbit/s for the first 2.6 years of the Spitzer cryogenic mission. Since Spitzer drifts away from the Earth at about 0.12 AU per year, the data transmission rate on the HGA decreased as a function of time, and the downlink strategy had to change to accommodate this by lowering the downlink rate and adding arrayed DSN dishes. The two low gain antennae (LGA) gave wide angle coverage but they only supported downlink at 44 kb/s at the beginning of the mission and at the end of the mission they were only capable of carrier-only signals. The LGA were used in safe and standby mode, but were not normally used to transmit science data during routine science operations. It was also possible to command Spitzer "in the blind" by sending commands to the spacecraft though the LGA if necessary.

Because of the location of the HGA, it was necessary to stop observing and point the telescope in the anti-Earth direction to downlink the science data though the antenna fixed to the bottom of the spacecraft. Depending upon the details of the observations that are scheduled, Spitzer produced ~1 to 6 Gbits of (compressed) science data during 12–72 hours of observing. During the cryogenic mission, Spitzer collected data for about 12–24 hours and then spent 0.5–1 hour downlinking the data. The scheduling system predicts the compressed data volume that is generated during each downlink and schedules the downlink contact time accordingly. The downlink periods are also used for some spacecraft maintenance activities (such as dumping angular momentum) and for uplinking commands. If low volumes of data are being generated, longer periods of time between downlinks may be used.

At each downlink opportunity, Spitzer attempted to transmit all the data in the mass memory. All data was stored onboard the spacecraft until it was confirmed to be on the ground safely. Any data that the ground had not confirmed as received was retransmitted at the next downlink pass. It was anticipated that some data could be missed at any pass, and it sometimes took several passes before the ground received all the science data for a given PAO. At the beginning of the mission downlinks were planned so that all data on board could be transmitted during the next downlink and the retransmit feature was used during anomalous situations. After October 2013 the distance to the spacecraft was so great (up to 1.77 AU) that the downlink rate had to be lowered to 550 kB/s and this retransmit feature was used on a regular basis during normal operations. The schedulers would plan for the telescope to take more data then could be downlinked during the next pass and store it onboard the spacecraft until a subsequent downlink.

Whenever the HGA was used for downlink, it was also possible to uplink commands and files to Spitzer. Normally ~3 to 5 communication periods per week were used to send up all the sequences and information needed to support the next upcoming week of observations. No communications with Spitzer were planned outside the scheduled downlink sessions.

The downlink strategy had little impact on observation planning with Spitzer in the cryogenic mission. It was one component in determining the maximum length of an Astronomical Observing Request (AOR)(a filled in AOT, defining a Spitzer observation), but the necessity for instrument maintenance operations and pointing system calibrations on shorter than 12 hour time scales constrained the maximum AOR length more tightly than the downlink schedule. A 12 to 24 hour interval between downlinks does imply that it can be a day or longer before science data are available on the ground after an observation is complete.

During the warm mission only 2 of 4 channels of the IRAC camera were operational, which cut the data volumes generated by IRAC in half. In addition the IRAC sub array mode, which was used for high precision photometry light curves (mostly of exoplanets), did not store the readout from the entire chip and could had extremely low data volumes, depending on the duration of the observation and the frametimes used. This allowed for much longer PAOs (24-72 hours) and made longer observations possible. Waivers were granted for these larger gaps in the instrument maintenance activities, and the pointing system calibrations were deferred until after the long observations, and then executed in bulk (e.g. after a 36 hour observation, three were executed back to back).

The uplink strategy did not directly affect observation planning in the cryogenic mission, but it drove the time scale on which changes to the stored science schedule and its contents can be made (e.g., for a ToO). In the warm mission, a minimum number of downlinks per week had to be scheduled to provide enough uplink opportunities.

During the warm mission a microlensing campaign was executed each summer for 6 weeks in the years 2015-2019 that required coordinated observations between ground-based observatories and Spitzer. During this time the uplink strategy drove the observation planning and the schedule for the entire Spitzer project. For a normal week the scheduling team built the week starting approximately 5 weeks in advance of execution. Two weeks were budgeted for reviews and fixes to the week, and it was uploaded to Spitzer in the week before it was set to execute (see section 4.2.1.4 “Scheduling Methodology” for more information). Microlensing events are on the order of a couple of weeks long, but Spitzer’s distance from Earth meant that it alone could obtain a parallax measurement for the ground-based events, if the usual scheduling process could be expedited. In the end, each week was built according to the usual process with a placeholder AOR

placed in the schedule once every 12 hours for the six weeks each summer that the galactic bulge (where the number of microlensing events is highest) was visible to Spitzer and Earth simultaneously. Special downlinks with backup dishes at highly prescribed times were negotiated with the DSN, with uplinks on Wednesday and Thursday afternoons. The microlensing team sent their targets, based on the ground-base observations, to the Spitzer Science Center by 8am on Monday morning, and the placeholder AORs were replaced with the microlensing AORs, and then the week was rebuilt, reviewed, modeled and approved by late Tuesday afternoon, uplinked to the spacecraft during the downlinks on Wednesday and Thursday, and started executing onboard Thursday afternoon. The process was successfully executed each time, and none of the weeks with the placeholder AORs were ever flown.

3.5 Sky Visibility

3.5.1 Solar Orbit

An important innovation enabling Spitzer to accomplish ambitious scientific goals at a modest cost is its Earth-trailing heliocentric orbit (shown in Figure 3.5), in which the observatory drifts away from Earth at the rate of ~ 0.12 AU/year. This separation from the Earth as a heat source substantially helped prolong the coolant lifetime by supporting an operating regime in which most of the cryogen is used to take up the power dissipated by the detector arrays, rather than lost to parasitic heat loads. In addition, this orbit has less-constrained visibility, compared to what would have been the case in a near-Earth orbit, allowing all parts of the sky to be visible for at least two extended periods each year and some zones to be visible continuously.

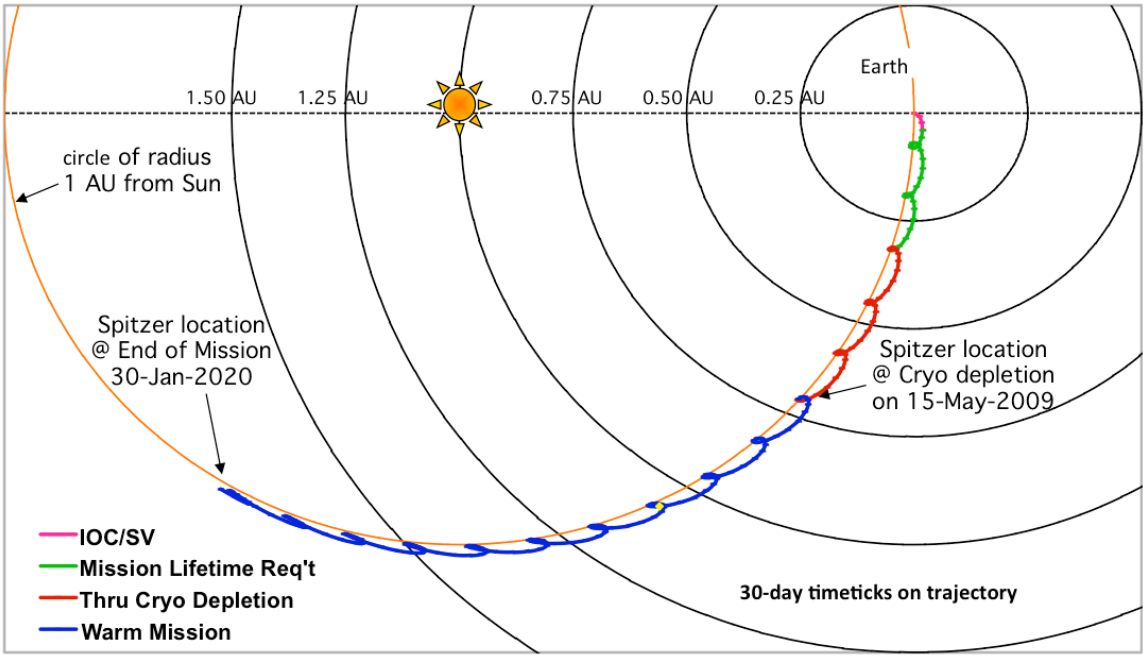

Figure 3.5: Spitzer's solar orbit projected onto the ecliptic plane and viewed from ecliptic North. In the rotating frame, the Earth is at the origin and the Earth-Sun line is defined as the X-axis. "Loops" and "kinks" in the trajectory occur at approximately 1-year intervals when Spitzer is at perihelion. Spitzer's orbit is also slightly inclined with respect to the ecliptic.

3.5.2 Pointing Constraints

Spitzer's view of the sky was limited by two hard pointing constraints, illustrated in Figure 3.6 and (in a different fashion) in Figure 3.7:

- The angle between the boresight and the direction of the Sun may never be less than 82.5º. (NB: this was updated in early 2004.)
- The angle between the boresight and the direction of the Sun may never exceed 120º.

The area defined by these hard constraints is called the Operational Pointing Zone (OPZ). In addition, some bright objects (such as the Earth) are normally avoided, because they would degrade the quality of the observation, due to direct exposure or stray light, but this is not a strict constraint (see section 3.5.6 and Appendix A). Note that the definition of the OPZ precludes observing Mercury or Venus with Spitzer. A second-order effect on the OPZ is provided by the limited roll angle of Spitzer around the Y-axis (see Figure 3.4), which is just ±2º.

Figure 3.7 shows the actual pointings of the observatory for one day in the life of Spitzer. Note the locations of the OPZ and how it constrains where the telescope actually pointed on that day.

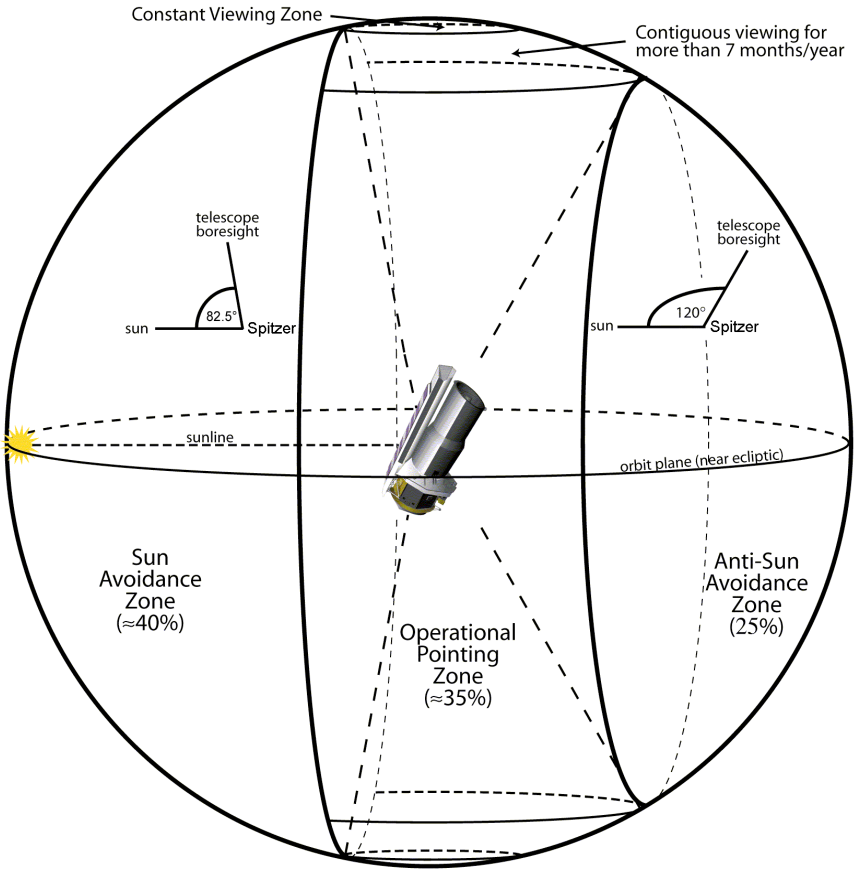

Figure 3.6: The main geometric observing constraints form an area called the Operational Pointing Zone (OPZ).

As the mission progressed, the pitch angle of the boresight relative to the sun when it was communicating with Earth gradually increased as Spitzer's distance to the Earth increased (see Figure 2.5). In December of 2013 this angle exceeded the edge of the OPZ (in the anti-sun direction, fortunately!) in order for the high gain antenna to be pointed at Earth. In order to continue to operate the spacecraft the onboard OPZ checks were disabled before each downlink to Earth.

Once the spacecraft was pointed outside the OPZ, it was no longer power-positive when downlinking to Earth and the onboard battery was used to power the spacecraft until it could be returned to a pitch angle within the OPZ. In October of 2015 the pitch angle of the science for two hours following each of these downlinks was restricted to 82.5 to 100 degrees so that the solar panels were approximately normal to the sun and recharged the battery faster. At the time of decommissioning the boresight/sun angle was 144.6 degrees, which was 24.6 degrees outside of the OPZ. Downlinks had a maximum duration of 140 minutes so as not to deplete the battery too far (the maximum battery depletion during a downlink measured was 53% (47% state of charge). Since the round trip light time to at this point Spitzer was 29 minutes and 32 seconds the downlinks also had a minimum duration of 120 minutes so that there was enough time to send and receive confirmation of sequences uplinked to the telescope.

3.5.3 Viewing Periods

The amount of time during the year any particular target is visible depends primarily on the absolute value of its ecliptic latitude (Figure 3.8). As seen in Figure 3.6, Spitzer's instantaneous window of visibility on the celestial sky forms an annulus (the OPZ), perpendicular to the ecliptic plane, of ~40º width and symmetrical with respect to the Sun. This annulus rotates with the Sun over the period of a year; the edges of the OPZ move along the ecliptic at about 1º/day as Spitzer orbits the Sun. For an object near the ecliptic plane, the length of the visibility period is ~40 days twice a year (modulo periods when undesired bright moving objects are also present and bright object avoidance has been selected; see section 3.5.6). The visibility periods increase to ~60 days twice/yr at an ecliptic latitude of ~45º, ~100 days twice/yr at latitudes ~ 60º, then becoming a single long window ~250 days long for latitudes near 60-70º, finally reaching constant viewing near the ecliptic poles. About a third of the sky is visible to Spitzer at any time. Figure 3.9 illustrates how the total number of days of visibility varies over the sky in three coordinate systems.

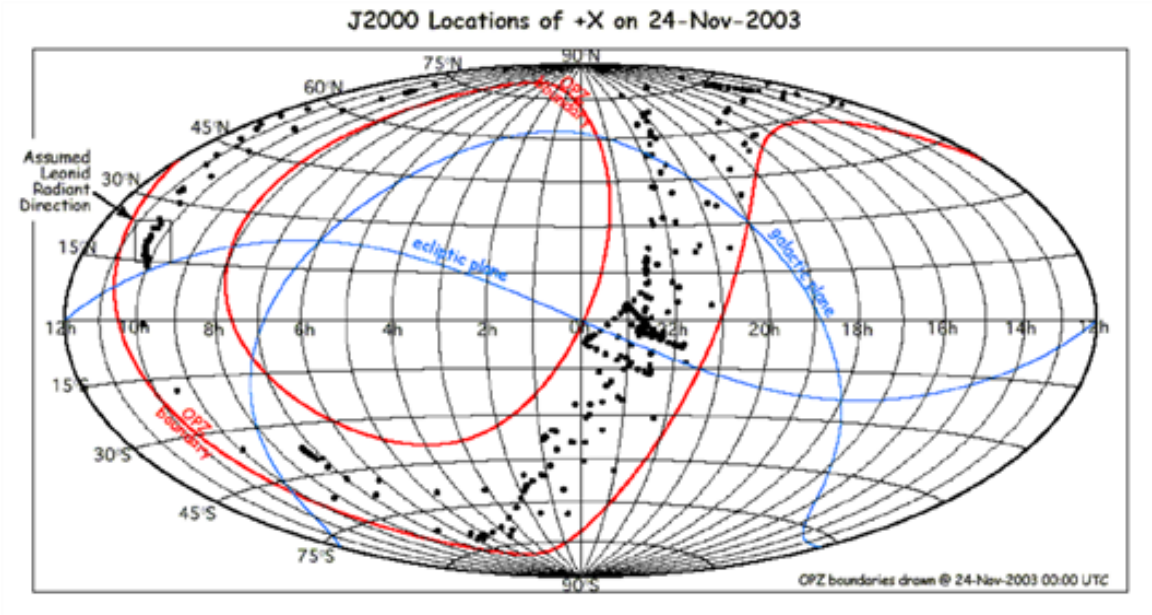

Figure 3.7: OPZ boundaries for 24 Nov 03 (0h UTC), with dots representing the actual locations of the telescope boresight for the subsequent 24 hours.

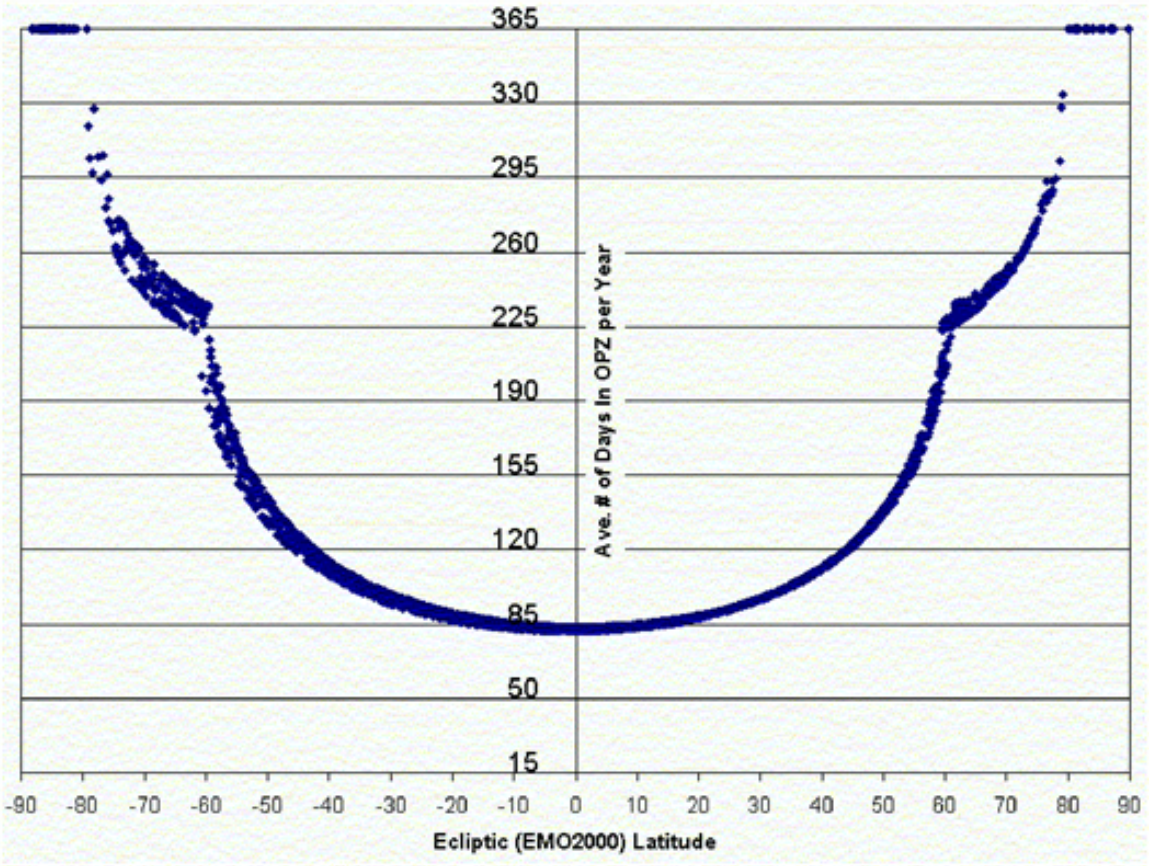

Figure 3.8: Variation of length of visibility period as a function of ecliptic latitude for all of the targets in the April 2003 ROC. (This figure is provided as indicative of the general concepts, despite the fact that the ROC has changed substantially since April 2003.)

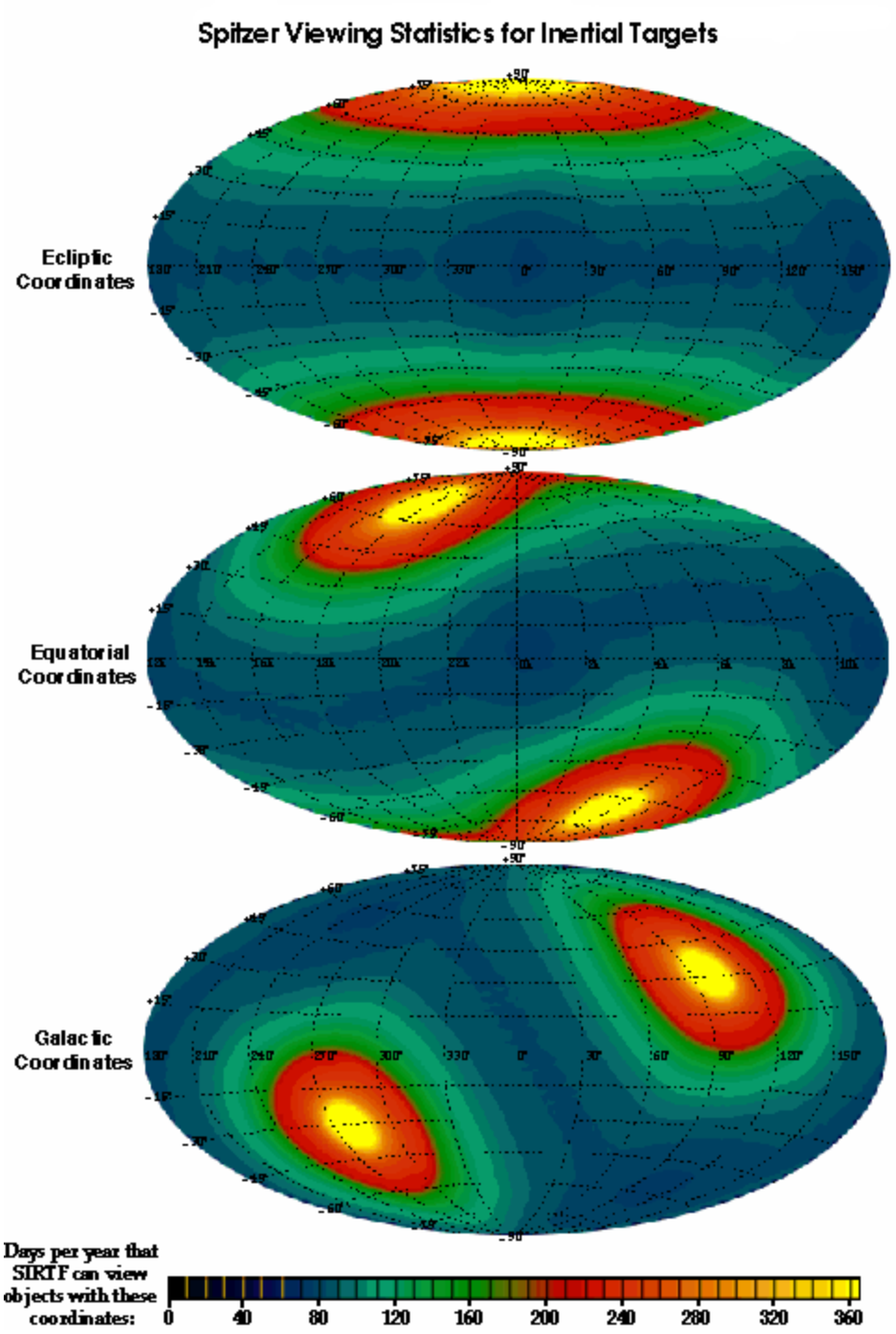

Figure 3.9: Total days of visibility per year in equatorial, ecliptic and galactic projections.

3.5.4 How Visibility Evolves with Time

Figure 3.10 illustrates the zone of visibility in equatorial coordinates for four specific dates during the first year of operations. Note how the sky passes into and out of visibility as the calendar date advances. Each set of contours shows the available and forbidden zones on a particular date (in this plot, 1 Sep 2003, 1 Dec 2003, 1 Mar 2004, and 1 Jun 2004). On each date, there is a forbidden zone in the anti-Sun direction, as well as a second, more extended-looking forbidden region on the side of the spacecraft towards the Sun; the Sun-ward forbidden region is in the center of the plot on 1 Sep and on the edges for the 1 Mar plot. Note that even targets at high declinations may fall in the forbidden zones part of the time, although objects at extreme declinations are generally visible for most of the year.

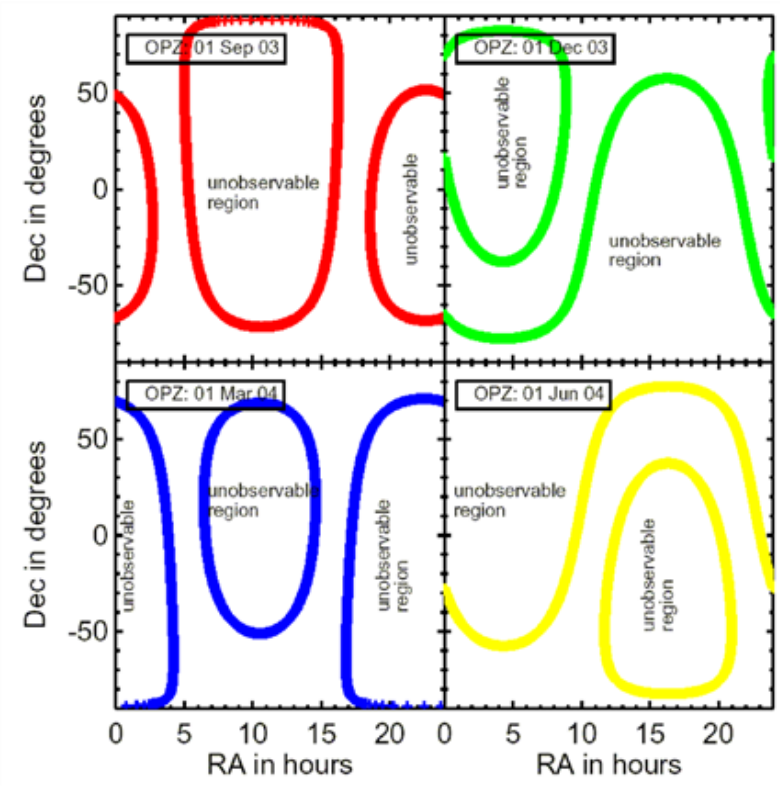

Figure 3.10: Example of time evolution of visibility zones over a year; see text.

3.5.5 Orientation of Focal Plane and Slits against the Sky

Spitzer had very limited ability to rotate the focal plane of the telescope. At any given time, the center of the sunshade (X-Z plane; see Figure 3.4 3.4) was always kept within ±2º of the Sun. This limited freedom in the "roll" angle was used to maintain a consistent orientation for long observations (AORs) and was not selectable by the observer. For each target, the orientation of the focal plane on the sky is a function of the position of the spacecraft along its solar orbit (i.e., the date of observation) and of the ecliptic latitude of the target. Targets in the ecliptic plane have only two possible focal plane orientation angles which are at 180º with respect to each other. Elsewhere in the sky, the focal plane has two ranges of orientation angles.

Science instrument aperture orientation within the focal plane is physically fixed. Because the spectrometer slits have quite different orientations within the focal plane (see Figure 3.1), this could be particularly limiting for IRS observations, but it also affected mapping with MIPS and IRAC.

3.5.6 Bright Object Avoidance

No object outside the solar constraint zone posed a threat to instrument safety. However, an observer may have wished to avoid observing the Earth and other bright moving objects to avoid compromising observations of faint targets. Therefore, the visibility windows calculated by Spot (the observation planning software: see section 4.5.1) avoided certain bright moving targets by default, although the observer could choose to override the default.

With bright object avoidance turned on (the default), the visibility windows calculated for both inertial and moving targets excluded regions of time when the positions of (a) the Earth and Moon, and (b) a fixed list of bright moving objects (e.g., Jupiter, Saturn, bright asteroids) coincide with the target position. The visibility windows was trimmed to delete any time periods when the Spitzer target is within 7º of the Earth or Moon and when the target is within 30 arcminutes of the other bright objects. Earth-Moon avoidance was only an issue early in the mission. As Spitzer moved farther away from the Earth, the Earth fell into the solar avoidance zone. The complete list of the bright moving objects is in Appendix A. The observer may have chosen to override the default (a) Earth/Moon or (b) other bright object avoidance. For example, to observe Jovian satellites, one would turn off (b) and leave (a) in effect.

3.6 Operational Constraints – Instrument Campaigns

Spitzer could operate only one science instrument at a time, so observing was divided into dedicated instrument campaigns typically lasting from 7–21 days. Once the campaign plan for a particular observing cycle (see section 3.1) ("Baseline Instrument Campaign," or BIC) had been established, it was published on the SSC website. Minor changes in the instrument campaign plan in response to changes in the DSN schedule, on-orbit anomalies, highly time-constrained observations, and changes to the SODB may have been made. Updated BICs were posted regularly on the SSC website.

There was a significant overhead associated with changeover from one instrument to another, due to the need to perform routine calibrations and engineering activities at the time of switch-off and switch-on. There were also performance limitations in some observing modes immediately following an instrument changeover. For example, the IRAC electronics stabilized after a warm-up of ~1/2 hour after switch-on. In addition, there was a modest reduction in pointing accuracy following a change between IRS/MIPS (which share common warm electronics) and IRAC, due to thermal distortion when the heat load is shifted on the spacecraft.

In order to achieve the required mission observing efficiency and ensure good performance, instrument changeovers were made as infrequently as possible without sacrificing science needs. The best balance between efficiency and schedule flexibility was achieved by using each instrument for several (~7–21) days at a time. This generally permitted long mapping projects, as well as highly time-constrained observations. An instrument campaign could be interrupted in

order to perform urgent ToO observations, with the proviso that it had to use the instrument then in use.

The instrument campaigns typically occurred in the order IRAC-MIPS-IRS, which conserved helium and minimized the effects on pointing performance described above. Observations requesting MIPS followed immediately by IRAC were not feasible under this scheme. The length of these campaigns was determined by the relative fraction of observation requests in the approved programs, and changed from cycle to cycle.

During the warm mission only the IRAC instrument was operating. It was cycled on and off only twice between May 2009 and January 2020, both times due to anomalies.

3.7 Pointing Capabilities

3.7.1 Pointing Control System

The PCS included the hardware and flight software necessary for precision telescope pointing, stabilization, slewing, tracking, and safe mode functions. The PCS performed the initial attitude acquisition of the spacecraft following launch vehicle separation. It provided periodic boresight calibration for the telescope relative to the star trackers on the spacecraft. The PCS provided the capability for both rapid large angle slews and small maneuvers to place and reposition science targets within the science instrument apertures; it maintained the solar array orientation toward the Sun; and, it pointed the high gain antenna toward Earth for downlink. The PCS also contained Wide Angle Sun Sensors (WASSs) that act as a second check on the spacecraft orientation to ensure that the hard pointing constraints (see section 3.5) are not violated. High-level fault protection would have placed the telescope in a safe mode if a violation was detected. The performance numbers presented in this and the following sections are based on our present understanding and measurements of the on-orbit PCS performance.

The PCS was a celestial-inertial, three-axis stabilized control system. A high performance star tracker/inertial reference unit (ST/IRU) package provided attitude determination and reconstruction capabilities. On-board pointing commands and variables used the J2000 coordinate system. Reference to the J2000 celestial sphere was implemented within the ST through autonomous identification of stars carried in an on-board catalog of 87,000 Tycho stars down to 9th visual magnitude. [The on-board catalog actually used the ICRS coordinate system, so, in fact, the on-board pointing system is really ICRS. However, the differences between ICRS and J2000 are so small (≤120 mas) that no conversions are made, and Spitzer is effectively considered to use the J2000 coordinate system.]

The ST was used to point an instrument boresight to a desired location on the sky with an initial accuracy of at least 0.5 arcsecond (1σ radial). The ST field of view is 5°×5°, which ensured that Spitzer can point to any part of the sky and have the ST meet its pointing requirements. Typically 40 stars were used simultaneously. The gyros provided pointing stability when not using the ST as a pointing reference; the pointing drift derived from the gyros was <3 mas/sec over 8 hours. The drift rate when using the IRU-only mode should generally be better than 1 mas/sec over 200 seconds.

All telescope pointing was defined and calibrated relative to redundant PCRSs located in the focal plane. During the course of the mission, the PCRS was periodically (about every 12 hours) used to calibrate the telescope-to-star tracker boresight alignment that may drift due to thermo-mechanical effects. Each PCRS detector is a Si PIN photodiode array divided into two 4×4 subarrays for redundancy. Each pixel is 250 μm square, with a plate scale of 10 arcseconds per pixel. The PCRS calibration measured the star position with an accuracy of 0.1 arcseconds (1σ per axis), and was sensitive down to 10th visual magnitude at a wavelength of 550 nm.

Spitzer also has WASSs (Wide Angle Sun Sensors), which measure the Sun's position with respect to the spacecraft. These sensors were used during initial attitude acquisition after launch, as well as for Sun avoidance, fault protection, and safe mode during the mission. Each wide-angle Sun sensor provides a field of view of 2π sr with an accuracy of ±0.1° at null. They were placed at the top and the bottom of the solar panels to maximize the coverage, with their boresights aligned to the spacecraft Z-axis. After the pitch angle of downlinks exceeded operational angle of the WASSs in September of 2016, they were disabled before each downlink to Earth. After the downlink completed, the spacecraft was pointed to a spot in the continuous viewing zone (CVZ) near the north ecliptic pole before fault protection were re-enabled, and then science observations could recommence.

Four reaction wheels provided the primary control actuation for all modes of operation. They were mounted in a pyramid orientation about the X-axis; each canted at 30° towards the X-axis. Over time, angular momentum accumulates in the reaction wheels, due primarily to the small offset between the center of mass and the center of (radiation) pressure. Unlike an observatory in low Earth orbit, which can dump this momentum magnetically, Spitzer has a Reaction Control System (RCS), which used cold nitrogen gas thrusters to provide the reaction wheel momentum unloading capability. Opportunities to dump momentum were scheduled approximately every 12 hours, but used only if sufficient momentum had accumulated in the reaction wheels. The nitrogen supply was sufficient to accommodate the entire mission lifetime from launch to decommissioning with room to spare.

On-orbit measurements show that the PCS is capable of slewing the telescope 180° in 900 seconds, 1° in 60 seconds, and 1 arcminute in 6 seconds, while maintaining its inertial pointing knowledge. These times include the acceleration and deceleration of the telescope, but do not include the time it takes for the PCS to stabilize after the slew has completed. The pointing system had several operating modes, and the AOTs are designed to use the pointing mode most appropriate for each observing mode. Settling time varies with operating mode and slew magnitude. For IRU-only slews, slews less than 30 arcseconds settle to within 0.2 arcseconds rms within 10 seconds. (Settling may have taken longer in some cases.) The AOTs made use of on-board slew completion and stabilization indicators to proceed with the observation as soon after a slew as is possible. Note that the time required for small slews, dithers, offsets, settling, etc., within an AOR is considered part of the observation.

3.7.2 Pointing Accuracy and Stability

The blind pointing accuracy was the same as the on-board attitude knowledge, <0.5 arcseconds (1σ radial rms) with a stability of <0.1 arcseconds (1σ radial rms over 200 sec). In the incremental pointing mode, the PCS performed controlled repositioning of the boresight with an offset accuracy usually no worse than 0.2 arcseconds and less than 0.6 arcseconds for across angular distances of up to 30 arcminutes. This accuracy was sufficient to move a source from the IRS Peak-Up array to one of the spectrometer slits. MIPS observers should note that the initial

blind pointing accuracy for the 160 micron array was expected to be significantly worse than for the shorter wavelengths (~3.9 arcseconds). See the MIPS Instrument Handbook for more information.

3.7.3 Scanning Stability and Performance

Spitzer could execute linear scans at selected rates from 0.01 arcseconds/second to 20 arcseconds/second. The MIPS Scan Map mode used rates from 2 arcseconds/second to 20 arcseconds/second.

3.7.4 Tracking Capabilities

Spitzer does not have a true tracking capability for Solar System Objects (SSOs). However, Spitzer simulated tracking by scanning in linear track segments at rates up to 1 arcsecond/second. The linear track segments are linear in equatorial coordinate space; they were commanded as a vector rate in J2000 coordinates, passing through a specified RA and Dec at a specified time.

The SSO ephemerides were maintained on the ground, rather than on-board Spitzer, but an observer may specify flexible scheduling constraints, and the linear pseudo-track specification (start point, rate and direction, in equatorial J2000 coordinates) was calculated at the time of scheduling. The observation was executed at the scheduled time (within a window of +3, -0 seconds), and the PCS follows the track as specified, assuming the given start point corresponds to the time given in the track command. All other PCS movements could be superposed on a specified track, including dithers and scans.

PCS measurements indicate that the blind track acquisition accuracy was ≤ 0.5 arcseconds, independent of the track rate, which is consistent with expected performance on fixed targets. The track stability was better than scan mode requirements: ~0.5 arcseconds in 1000 seconds. The offset accuracy during tracking was better than ~0.55 arcseconds, also consistent with the required performance on fixed targets.

3.7.5 Pointing Reconstruction

Pointing reconstruction refers to the post-facto determination of where the telescope was pointed with a greater accuracy than was known by the flight system. Spitzer had a requirement to perform pointing reconstruction to 1.4 arcseconds. Based on in-orbit results, Spitzer met this requirement, except for observations scheduled immediately after an instrument changeover (in which case the inaccuracy may be as much as ~2 arcseconds). The nominal pointing is reported in the data products. Based on post-BCD processing and comparison of extracted sources with 2MASS sources, users will receive data with IRAC data pointing reconstruction generally <1 arcseconds, and MIPS scan pointing reconstruction generally <1.5 arcseconds, with respect to the 2MASS coordinate system. Relative pointing (relative separation of two objects within an AOR) is good to <0.5 arcseconds.

3.8 Optical Design

The telescope is a Ritchey-Chrétien design, known from on-orbit measurements to be diffraction-limited at 5.5 microns over the IRAC field of view, and expected to be diffraction-limited at 6.5 microns over the entire field of view. The 85-cm diameter primary mirror and the rest of the telescope structure were fabricated entirely of beryllium, utilizing advances in optical design, testing, and fabrication to produce a lightweight telescope that operates at cryogenic temperatures. The optical design parameters for the telescope are summarized in Table 3.3 below. The telescope configuration is shown in Figure 3.11.

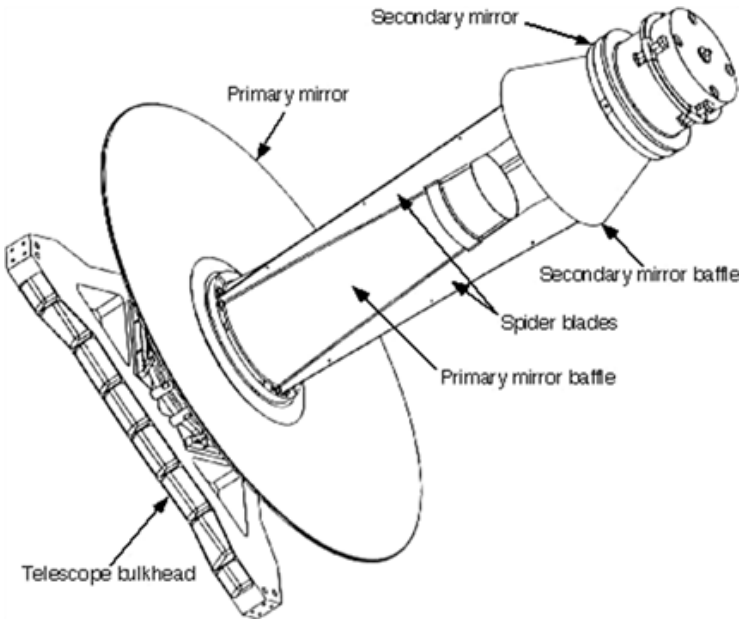

Figure 3.11: Spitzer Telescope Assembly.

Table 3.3: Telescope Configuration.

Optimal Parameter Description	Value at 5.5 K
System Parameters:	
Focal Length	10,200 mm
Focal Ratio	f/12
Back focal length (PM vertex to focus)	437 mm
Field of View (diameter)	32.0 arcmin
Field curvature radius	140.5 mm
Wavelength coverage	3 μm–180 μm
Aperture Stop:	
Location	Edge of primary mirror
Diameter of OD obscuration	850.00 mm
Diameter of ID obscuration	320.00 mm
Linear obscuration ratio	0.3765
Primary Mirror (hyperbola)	
Radius (concave)	-2040.00 mm

Conic constant Clear aperture Focal ratio	-1.003546 850.00 mm f/1.2
Secondary Mirror (hyperbola) Radius (convex) Conic constant Clear aperture (OD)	 -294.343 -1.531149 120.00 mm
PM to SM spacing (vertex to vertex)	887.528 mm

The telescope employs a single arch primary mirror, which reduces mass. The primary mirror is supported on three bipod flexures relatively close to its axis. The spider blades, primary mirror baffle, and secondary mirror baffle are integrated into a one-piece, relatively small diameter metering tower extending through the central hole in the primary mirror.

3.9 Optical and Thermal Performance

3.9.1 Surface Accuracy

The Ritchey-Chrétien design minimizes spherical aberration and coma over large fields of view. Field curvature varies quadratically with field angle. Similarly, the rms wavefront error at best focus varies quadratically with field angle and equals 0.52 waves ($\lambda = 0.6328$ microns) at the edge of the field. Essentially all of this error is due to astigmatism.

The surface figure for the primary mirror was measured at cryogenic temperatures to be 0.067 microns rms over the entire clear aperture, meeting the specification of 0.075 microns rms (Figure 3.12).

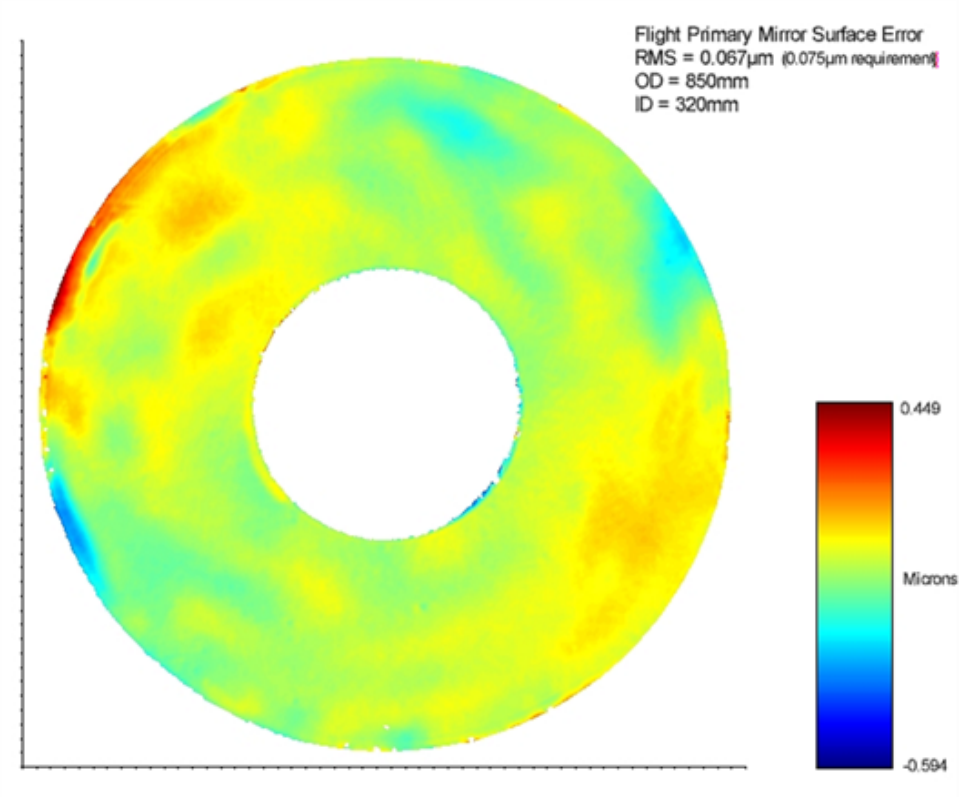

Figure 3.12: The deviations in the flight primary mirror surface. The RMS error was measured at cryogenic temperatures to be 0.067 microns rms over the entire clear aperture, meeting the specification of 0.075 microns rms.

3.9.2 Wave-front Errors

The telescope was required to provide a beam to the telescope focal surface that is diffraction limited (transmitted wave front error < λ /14 rms) at 5.5 microns over the entire field at operating temperature. At a wavelength of 3.5 microns, the telescope produced a wave front error of less than 0.13 λ rms over the IRAC field of view, and the image of a point source contains 45% of the encircled energy within a diameter of 2 arcseonds. The actual performance of the telescope is slightly better than the requirements; see the IRAC Instrument Handbook more information.

3.9.3 Throughput

The requirements for the telescope assembly are that it shall provide a minimum end-of-life throughput no less than that given in Table 3.4. Telescope throughput is defined as the ratio of energy from a point source reaching the telescope focal surface to the energy collected by an 85 cm diameter mirror. Factors that degrade telescope throughput are the central obscuration (including spiders), mirror reflectivity as a function of wavelength and losses due to contamination.

Table 3.4: Telescope Throughput

Wavelength (microns)	End of Life Throughput
0.55	> 0.18
3.5–6.5	> 0.70
6.5–10	> 0.73
10–20	> 0.74
20–200	> 0.75

3.9.4 Stray Light Rejection

The cryostat, telescope, multiple instrument chamber and science instruments are designed and baffled such that, at all wavelengths from 3.6 to 160 microns (center of passbands), celestial stray radiation and internal stray radiation:

- Do not, except for lines of sight near bright sources, increase by more than 10% the photon noise of the natural background in the direction of the line of sight of the telescope. This requirement implies that the combination of celestial stray radiation and internal stray radiation must be < 21% of the natural background at the instrument detector arrays.
- Display no gradients or glints in the celestial stray light that will increase confusion noise over natural levels or produce false sources.
- Do not significantly decrease the contrast of the first dark ring of the diffraction-limited point spread function.

The conformance of the Spitzer design to its stray light requirements was verified by analysis using the APART stray light analysis program and an analytical test source designed to approximate the brightest celestial source expected in each of Spitzer's wavelength bands. The actual scattered light performance of the Spitzer telescope was characterized on-orbit during the early parts of the mission and throughout nominal operation of the telescope. In some cases, there are modifications or caveats to the requirements above. Discussion of stray light as it pertains to each instrument is covered in the instrument chapters later in this document.

A useful output from the stray light analysis is a set of predicted point source transmission curves. The point-source transmission function (PST) is the inverse of the ratio of the flux density ($W/m^2/Hz$) of an off-axis source to the flux density at the telescope focal plane due to light scattered from that source. The separate PST curves in Figure 3.13 refer to different azimuthal locations of the celestial point source. An azimuth of 0º refers to the anti-Sun direction. The differences among the azimuths are mainly due to the changing illumination of struts supporting the secondary mirror. Figure 3.14 shows the variation as a function of wavelength.

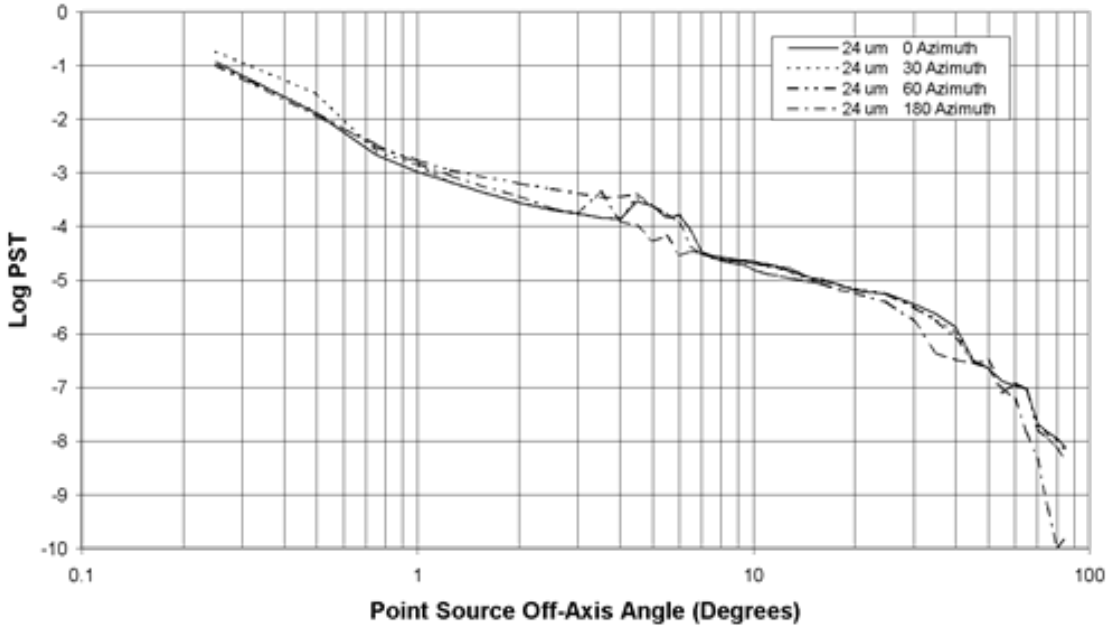

Figure 3.13: Theoretical PST for 24 microns off-axis as a function of azimuth.

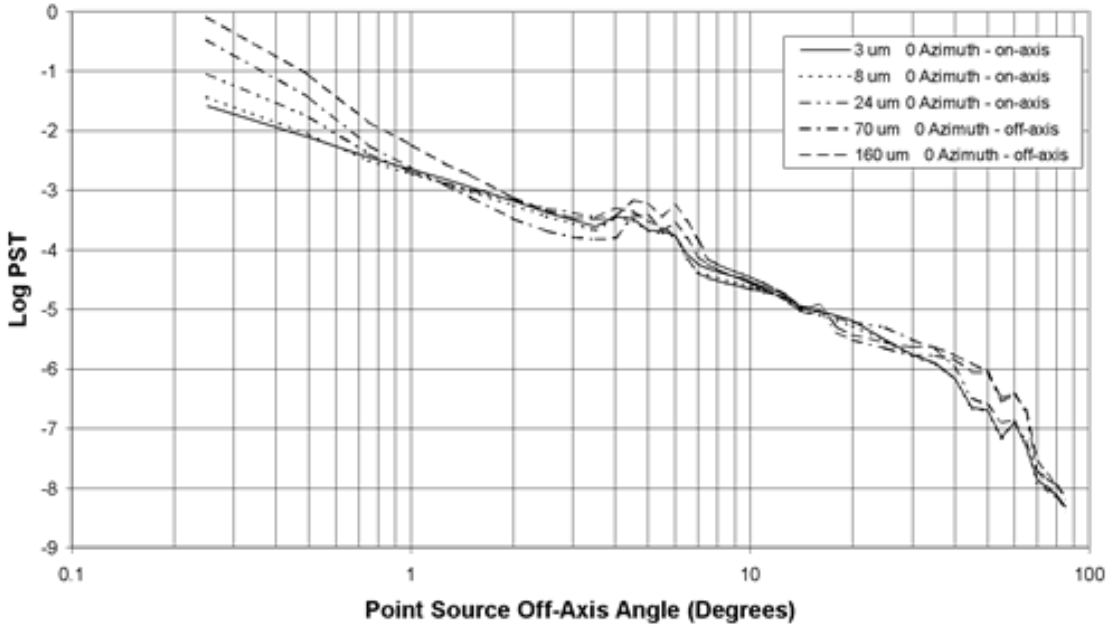

Figure 3.14: Theoretical PST as function of wavelength for fixed azimuth on-axis.

These plots can be used to estimate the stray light contribution from a given source. For example, at 8 microns, Vega has a flux density of ~62 Jy. From Figure 3.14, the 8 micron PST at 1º off axis is ~2×10^{-3}, so the predicted flux density in the Spitzer focal plane due to Vega at 1º off axis is 120 mJy. [The natural background at 8 microns near an ecliptic pole is 5.3 MJy/sr, which is

imaged to a flux density of 5.3 MJy/sr x π /(4x12^2) = 2.9x10^4 Jy over the focal plane of the *f*/12 Spitzer telescope. The scattered light from Vega at 1º off-axis is far below the natural background. The first stray light trouble from Vega at 8 microns should come from the outer parts of its diffraction-limited PSF.]

3.9.5 Telescope Temperature/Thermal Background

During the cryogenic mission the telescope was cooled by helium vapor vented from the cryostat. The helium vaporization was driven by power dissipated by the Science Instrument cold assemblies. A supplemental heater is available to provide additional vaporization, if needed. The required telescope temperature and heat load drove the required helium flow rate. As discussed in section 3.4.1, the telescope was launched warm and gradually cooled by a combination of radiative cooling and helium boil-off to ~6 K during the first ~45 days in orbit. The telescope temperature varied between ~6 K and 12 K depending upon how much power is dissipated in the cryostat. The power thus dissipated depended primarily upon the science instrument in use; the "make-up" heater may be used to ensure that the telescope is maintained at ~6 K when needed for 160 microns observations.

During the warm mission the telescope and instruments were passively cooled by space. The thermal design of the telescope meant that without liquid helium coolant, the instrument chamber remained cold enough to operate the two shortest channels (3.6 and 4.5 micron) of the IRAC instrument. A supplemental heater was used to slightly heat the detector arrays to 28.5K so the temperature did not float and was under direct control.

3.9.6 Telescope Focus

Spitzer was equipped with a secondary mirror focus mechanism, which was operated both on the ground and on orbit. Prior to launch, the end-to-end image quality was measured on the ground and the mechanism was set to the position that was predicted to give optimal focus following in-orbit cool-down. During In-Orbit Checkout (IOC), it was found that the telescope focus point was about 1.85 mm above (toward the back of the primary mirror) the optimum focus position for the science instruments. Thirty-eight days after launch, when the telescope had become thermally stable, the secondary mirror was moved toward the primary mirror to bring the telescope into focus. The instruments are confocal, so that separate adjustment of the focus for each instrument was not necessary.

3.10 Focal Plane Layout

Figure 3.15 shows the actual location of the pick-off mirrors that feed the science instruments as viewed from above (looking down the boresight). The Y- and Z-axis directions are the same as the telescope coordinate system shown in Figure 3.4; the +X direction comes out of the page. Figure 3.15 shows the Spitzer entrance apertures as projected onto the sky and appears inverted compared to Figure 3.1, due to the combined effects of looking out from behind the focal plane and the projection of the sky onto the focal plane through the telescope optics. (To understand this inversion, recall the 3-D geometry and the fact that a Cassegrain telescope inverts its image.)

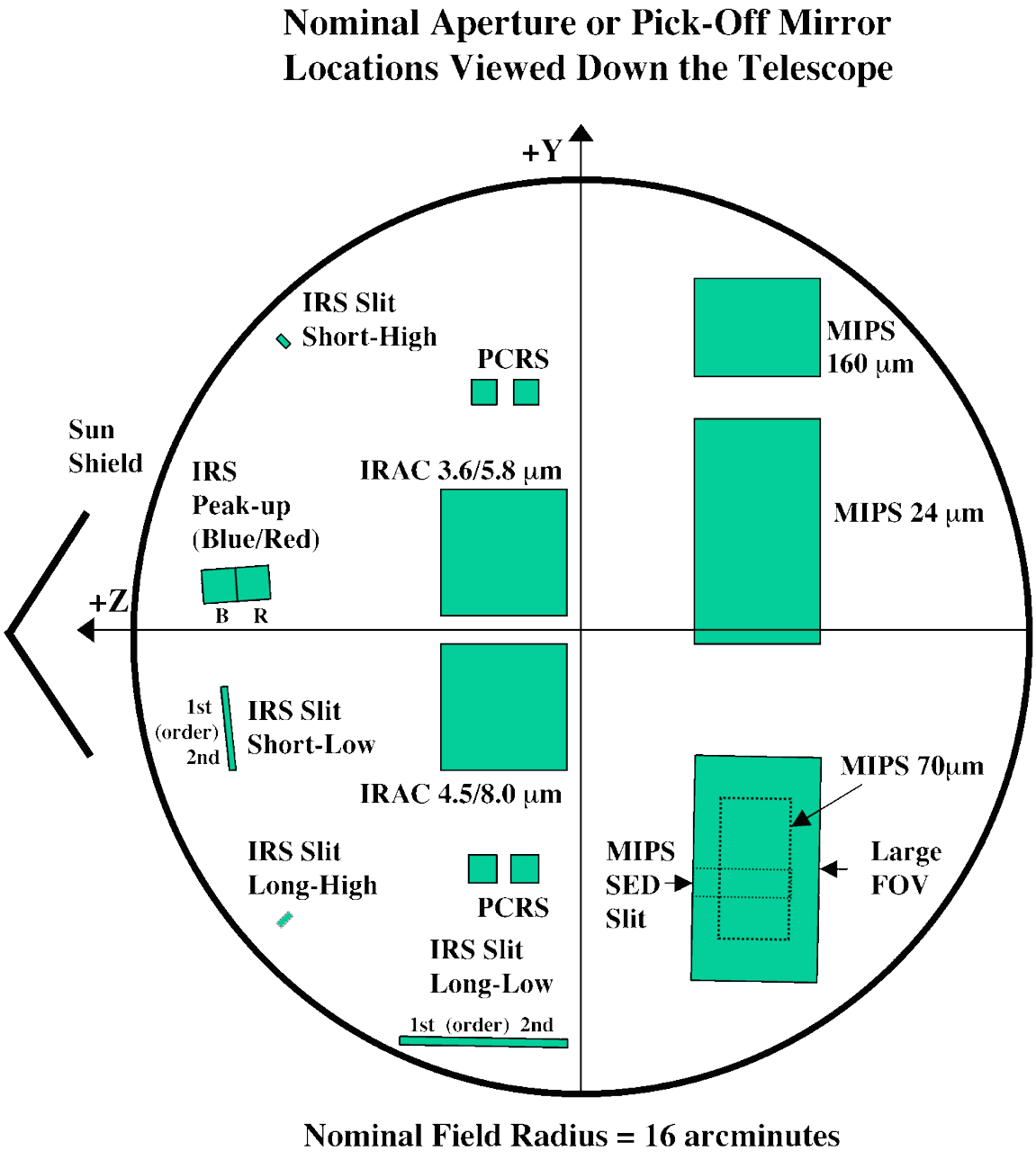

Note: This is an approximate mechanical layout of the focal plane as viewed from above. It is not a projection onto the sky.

Figure 3.15: Schematic view of Spitzer focal plane from above, looking down the boresight. The solar panel is on the IRS side of the spacecraft. This figure shows the region of the focal surface where the pick-off mirrors for each instrument are located. This is in contrast to where the apertures project onto the sky. See Figure 3.1 for comparison.

Table 3.5: Spitzer focal plane layout: approximate offsets from boresight to aperture centers.

Aperture	Z (′)	Y (′)
IRAC 3.6 μm	2.86	3.67
IRAC 3.6 μm subarray	4.97	5.88
IRAC 5.8 μm	2.86	3.61
IRAC 5.8 μm subarray	0.72	5.71
IRAC 4.5 μm	2.72	-3.05
IRAC 4.5 μm subarray	4.80	-0.92
IRAC 8.0 μm	2.75	-3.07
IRAC 8.0 μm subarray	0.65	-0.97
IRS SL 1st order	12.03	-2.79
IRS SL 2nd order	11.91	-4.09
IRS LL 1st order	4.41	-14.00
IRS LL 2nd order	1.21	-14.07
IRS SH	10.56	10.01
IRS LH	10.42	-10.23
IRS Red Peak-Up	11.63	2.00
IRS Blue Peak-Up	13.52	1.91
MIPS 24 μm	-6.72	4.25
MIPS 70 μm default	-6.53	-8.06
MIPS 70 μm fine	-7.10	-6.81
MIPS 70 μm default side A	-7.95	-8.11
MIPS 70 μm fine side A	-6.39	-6.71
MIPS 160 μm	-7.35	12.11
MIPS SED	-6.06	-9.44

Table 3.5 gives the measured offsets from the center of the field of view to the centers of the main science apertures. The values were determined post-launch based on the results from the focal plane mapping survey during IOC+SV.

Each of the fields of view that are used has a code that specifies the position in the focal plane. The uplink software uses the field-of-view index for commanding the target position, and the pipelines similarly use it to reconstruct where the telescope was pointing. These indices and field-of-view names appear in the headers of Spitzer data, and are listed in Table 3.6.

Table 3.6: Field-of-View Indices.

FOV name	FOV index
Telescope Boresight	1
PCRS 1A	4
PCRS 1B	5
PCRS 2A	8
PCRS 2B	9
IRS red peak-up FOV center	18
IRS red peak-up FOV sweet spot	19
IRS blue peak-up FOV center	22

FOV name	FOV index
IRS blue peak-up FOV sweet spot	23
IRS SL 1st order 1st position	26
IRS SL 1st order 2nd position	27
IRS SL 1sr order center position	28
IRS SL module center	29
IRS SL 2nd order 1st position	32
IRS SL 2nd order 2nd position	33
IRS SL 2nd order center position	34
IRS LL 1st order 1st position	38
IRS LL 1st order 2nd position	39
IRS LL 1st order center position	40
IRS LL module center	41
IRS LL 2nd order 1st position	44
IRS LL 2nd order 2nd position	45
IRS LL 2nd order center position	46
IRS SH 1st position	50
IRS SH 2nd position	51
IRS SH center position	52
IRS LH 1st position	56
IRS LH 2nd position	57
IRS LH center position	58
IRAC center of 3.6 and 5.8 arrays	67
IRAC center of 3.6 array	68
IRAC center of 5.8 array	69
IRAC center of 3.6 subarray	70
IRAC center of 5.8 subarray	72
IRAC center of 4.5 and 8.0 arrays	74
IRAC center of 4.5 array	75
IRAC center of 8.0 array	76
IRAC center of 4.5 subarray	77
IRAC center of 8.0 subarray	79
IRAC between arrays	81
MIPS 160 center	87
MIPS 160 large only	89
MIPS 160 small	91, 92
MIPS 24 center	95
MIPS 24 small	99, 100
MIPS 24 large	103, 104
MIPS SED	105, 106, 121, 122, 123, 125, 126
MIPS 70 center	107
MIPS 70 TP	109
MIPS 70 default small	111, 112
MIPS 70 scan	113
MIPS 160 scan	114
MIPS 70 default large	115, 116
MIPS 70 fine	117, 118, 119, 120, 124, 127

Chapter 4. Observatory Operations

4.1 Spitzer Science Center

The Spitzer Science Center (SSC) conducted the science operations for Spitzer, and was charged with 1) acting as an interface and advocate for users, 2) capturing and conducting the science program efficiently, 3) producing and securing the Spitzer science legacy, and 4) conducting public and scientific outreach for the Spitzer program. The SSC was located on the campus of the California Institute of Technology in Pasadena, California, USA.

In carrying out its charter, the SSC issued annual Calls for Proposals, organized science and technical reviews, selected observing programs based on a Time Allocation Committee review, and administered data analysis funding awards. The SSC provided tools for detailed planning of Spitzer observations and proposal submission, and offered Science User Support services. In addition, the SSC scheduled observations on the telescope, provided basic (pipeline) science data processing and data quality assessment, and created a public data archive of Spitzer observations.

4.2 Spitzer Science Operations Overview

4.2.1 The Life Cycle of a Spitzer Observation

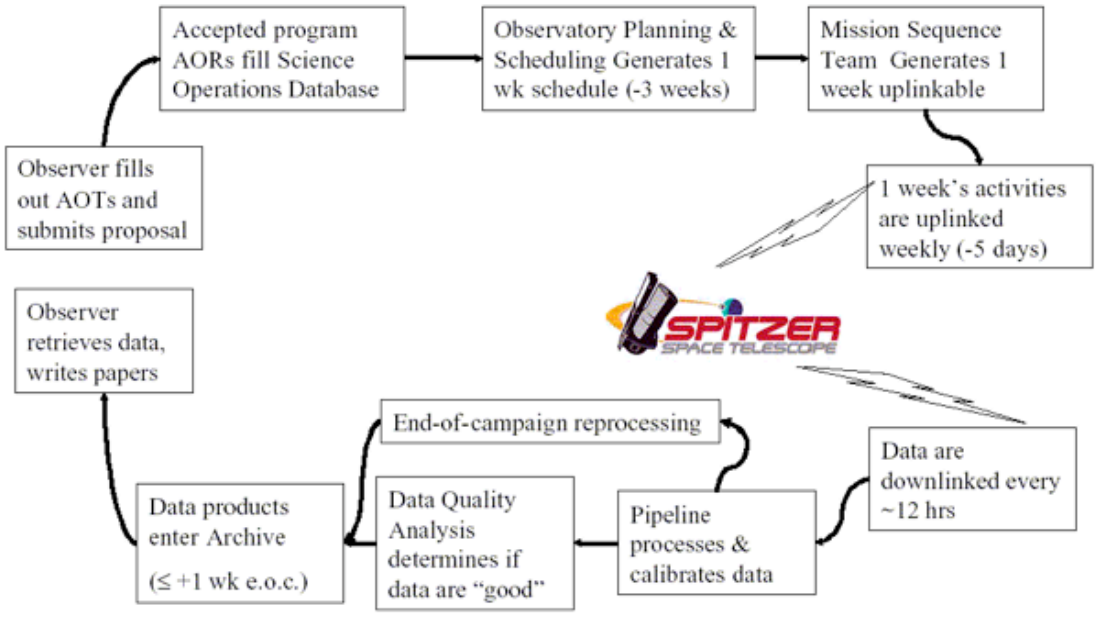

Figure 4.1: The life cycle of a Spitzer observation. The detailed definition of observations will occur at the time of each annual proposal solicitation.

4.2.1.1 Proposal Planning and Preparation

Figure 4.1 shows the basic stages through which a Spitzer observation passed. The process of defining a Spitzer observation starts with the choice of an astronomical target and the selection of one of the ten observing modes (Astronomical Observation Templates - AOTs). An SSC-supplied software tool called Spot was used to enter the target information and the observation details. After the AOT was chosen, Spot was used to enter all the parameters (e.g., integration time, choice of modules, etc.) needed to fully specify the observation. This process is called "filling out the AOT front-end." Spot also provided wall-clock time estimates for the total duration of observations. An observation which has been fully defined by supplying parameter values for an AOT is known as an Astronomical Observation Request (AOR), and is the basic scheduling unit for Spitzer.

4.2.1.2 Proposal Review and Selection

During the cryogenic mission General Observer (GO), Legacy Science, Archival Research, Theoretical Research, and Guaranteed Time Observer (GTO) proposals were solicited through yearly Calls for Proposals issued by the SSC. During the warm mission three more program types were added: Exploration Science, Frontier Legacy and Snapshot. The proposals were evaluated by topical science panels and Time Allocation Committees (TACs) consisting of members of the international astronomical community. The topical panels were grouped into six broad categories:

Extragalactic – distant universe
Extragalactic – nearby universe, local group (except stellar studies in nearby galaxies)
Galactic – brown dwarfs, circumstellar disks
Galactic – ISM, galactic structure, star formation, (plus stellar studies in nearby galaxies)
Galactic – evolved stars, compact objects
Planetary systems – extra-solar planets and our Solar System

Evaluation criteria for the proposals in order of descending importance were:

- The overall scientific merit of the proposed investigation and its potential contribution to the advancement of scientific knowledge.
- The extent to which the proposed investigation requires the unique capabilities of the Spitzer Space Telescope.
- The technical feasibility and robustness of the proposed observations.
- The extent to which the observations can be accommodated within routine Spitzer operations and the extent to which the overall science program enables an efficient use of the observatory.
- The long-term archival value of the proposed observations.
- The demonstrated competence and relevant experience of the Principal Investigator and any Co-Investigators as an indication of their ability to carry out the proposed research to a successful conclusion.

The TACs recommend lists of programs to the SSC Director, who was the ultimate selection official for all Spitzer research programs.

4.2.1.3 Scheduling

After the Time Allocation process has been completed, the programmatic information (Principle Investigator, title, abstract, etc.) and AORs of the approved proposals were loaded into a database known as the Science Operations Database (SODB), and were stored there in the form of a set of specific parameters and values. The AOR parameters were used by the software AOR/IER Resource Estimator (AIRE) to expand the set of parameters into a set of instrument and spacecraft commands which execute the observation on board Spitzer, as well as to provide extremely high fidelity estimates of execution time for the scheduling process. Observers also could access AIRE through Spot for their time estimates. The Spitzer planning and scheduling process produced observing schedules based on these resource estimates. After the content of the schedules had been approved and finalized, AIRE takes the AOR parameters and produces command product files which were then processed by the JPL Mission Sequence Team and finally uplinked and executed by Spitzer. *It is important to realize that the process of creating commands to carry out an observation based on the AOR parameters was done by software, not by support astronomers at the SSC.*

4.2.1.4 Scheduling Methodology

Observations were grouped into instrument campaigns, which are periods of several days during which only one instrument is used. Instrument campaigns vary in length as needed to accommodate the science program, typically running about 7 to 21 days. The planning and scheduling process included determining the optimum structure of instrument campaigns – called the Baseline Instrument Campaign Plan (BIC), and included tentative long-range planning of large, coherent programs or observations. This type of campaign planning occurred shortly after a new set of observations become available following solicitation, review, and selection (i.e., a Call for Proposals). The BIC was published on the SSC website once it was considered stable, but it was subject to change without notice, due to the need to respond to actual events on-orbit.

Spitzer scheduling was done using the LISP-based software SIRPASS which includes the traveling salesman algorithm GREEDY. After the BIC was set and long-range planning of highly constrained observations for the next three to six months was completed, the scheduling process then focused on the short-term scheduling of each week. At any one time there were about six weeks in the process – one week was being scheduled by the scheduler; a second week was being reviewed for schedule approval; a third week was in Pass 1, having had any adjustments applied after schedule approval; a fourth week was in Pass 2, having fixed any issues that came up in the Pass 1 review (many weeks did not need a Pass 2 review – the Pass 1 review was clean); a fifth week was having its commands uplinked to the spacecraft while a sixth week was executing on the spacecraft. Early in the mission a Pass 3 review was often required (occurring later in the same week as the Pass 2 review) but after several months of actually scheduling (and reviewing) most weeks were good to go at Pass 1 or 2. Only very rarely were Pass 3's needed. During the cryogenic mission there was one scheduler per week (6 people), by the end of the warm mission there were 3 schedulers. In general, Spitzer "weeks" run from Thursday to Wednesday and, during the cryogenic mission, could contain observations using more than one instrument.

Scheduling for a given week started about five weeks ahead of the actual start of execution of the week with the layout of the science instrument(s) calibrations and any spacecraft maintenance observations or activities. Then the science observations were pooled and inserted into the timeline, with various iterations/adjustments needed to optimize the slewing and remove or

minimize violations of observer requested scheduling constraints. This was the longest part of the process usually taking three to four days to complete. If an observation could not be scheduled within its observing constraint(s), due to a conflict with another science observation or with a spacecraft activity (including downlinks), the SSC would contact the observer to see if the constraint can be relaxed. If the constraint could not be relaxed the observation was removed from the current schedule and an attempt was made later to schedule it when the target was again visible to Spitzer.

Approximately three weeks before a schedule was been uplinked to the spacecraft, the list of scheduled AORs and their nominal execution times was published on the SSC website. An email was sent to the observer, notifying him/her that his/her observation had been scheduled. Once an AOR has been scheduled, only a significant anomaly (e.g., a missed downlink opportunity or a safing event) or a rapid-turnaround ToO could cause the schedule to change.

For five years (2015-2019) during the summer months Spitzer conducted a microlensing campaign to provide parallax measurements to microlensing events in the galactic bulge. During this time additional events were added to the usual build schedule. See the end of section 3.4.3 of this document for more details.

4.2.1.5 Scheduling Constraints for Science Reasons

The scheduling software was able to handle common types of constraints and logical linkages, such as those needed for periodic monitoring of a target. If a scheduling constraint was required, it was strongly recommended that the minimum constraint necessary to preserve the scientific goal of the observation(s) be applied. In general, larger timing windows and/or loose groupings were preferred to non-interruptible sequences of observations. For very long observations, strategies which permit independent scheduling of the component AORs were much preferred; this not only enhanced scheduling efficiency, but also made the observation as a whole much more robust against the failure of component AORs. As a general rule of thumb, groups of constrained AORs that occupied more than about half of the time period during which they can be scheduled were difficult to accommodate. For example, 100 hours of observations that must be done within a 100-hour period cannot be scheduled, whereas the same 100 hours of AORs may have been quite feasible if they can be scheduled anytime within a 200 hour period. The ability to be scheduled is further enhanced by making the observations shorter; 100 hours of 2-hour AORs constrained to a 120-hour period may be barely feasible, whereas 100 hours of 6-hour AORs cannot be scheduled in a time period shorter than 200 hours.

The following types of scheduling constraints are supported for both inertial and moving targets:

Timing Constraints

Timing constraints consist of defining a window or series of windows for the start time of an AOR. Absolute-time observations that will be executed at a specific time, or no more than 3 seconds later, can only be supported for moving targets. To specify an absolute time observation in a *moving target* AOR, set the open and close times for the timing window to be identical. Spitzer's scheduling architecture generally operates on relative time, so for inertial targets, the (inertial target) AORs will simply run in order. Timing constraints for inertial target AORs should be macroscopic (days, weeks, months), not microscopic (seconds, minutes, hours).

Relational Constraints

Relational constraints are ordering or grouping constraints that are applied to a group of AORs. There are four basic types of relational constraint supported by Spitzer:

Chain = Ordered Non-interruptible Group

A chain can be thought of as a list of AORs that must be executed consecutively in the order specified and without any other kind of activity intervening. Note that the total time for the entire ordered non-interruptible group cannot exceed the maximum time for an individual AOR; for longer observing sequences, an interruptible group must be used. This type of constraint might be used for an on/off source pair of observations.

Sequence = Ordered Interruptible Group

A sequence constraint is similar to, but less stringent than, a chain constraint. The AORs will be executed in the order specified and a duration in which they should be completed is specified. The sequence constraint should only be used when the science requires sequential ordering of the AORs. For AORs in which the order of observation is not important, a "group within" constraint (see below) should be used, instead of a sequence constraint.

Group-within

A group-within constraint specifies that a group of AORs will be executed within a specific length of time, but with no particular starting date/time constraint. Once the first AOR has been executed, the rest of the AORs in the group will begin within the specified time interval. They may be executed in any order within the time interval. This is similar to a sequence constraint, but the observations may be executed in any order.

Follow-on

This constraint forces a follow-on AOR to be scheduled within a given time after a precursor AOR. It can be thought of as a statement that Follow-On-AOR must be scheduled within Time-Window after the end of Precursor-AOR. The follow-on constraint can be used to prevent early execution of an observation when the success or content of the follow-on is dependent upon the successful execution of a precursor observation. This constraint could also be used for periodic observation of a target where the interval between observations is relatively short (hours to a small number of days). One AOR may serve as the precursor to more than one follow-on, but a follow-on may have only one precursor (e.g. one follow-on constraint can tie together only two AORs).

Shadow

The shadow constraint is a special case of the follow-on constraint, and is used to obtain background measurements for moving targets. The primary AOR is executed as specified. The shadow AOR will be executed to repeat the track of the primary observations. The selected AOR parameters must be identical in the two AORs. The shadow may be executed before or after the primary AOR. Note that the shadow does not re-observe the target at a later date, but rather the background of the primary observation. (As with all constraints, shadow observations must be strongly scientifically justified in the observing proposal.)

Timing and Relational Constraints can be combined. For example, a series of AORs used to obtain spectra of a comet over a long track which needed to be broken up into segments due to curvature, might be constrained as a chain with an associated timing constraint related to the acceptable range of solar elongations.

4.2.1.6 Pipeline Processing

After an observation had been scheduled and carried out, the resulting data were pipeline-processed, undergo a brief quality-checking process, and were placed in the Spitzer science archive and made available to the observer, usually within a week or two after the end of the campaign.

4.2.2 Data Products

Three levels of processed data were created: Level 0 (raw data), Level 1 (Basic Calibrated Data; BCD) and Level 2 (Ensemble data, also known as "post-BCD data"). Level 0 data are the unprocessed data, which have been packaged into FITS format. Level 1 data are single-frame FITS format data products, which have been processed to remove instrumental signatures, and which are calibrated in scientifically useful units. Level 2 data are higher-level products, and may include mosaicking, co-addition, or spectrum extraction. The data products are described in more detail in the Instrument Handbooks.

In general, the final calibration for an instrument campaign, which is typically about one to three weeks in duration, is based upon calibration observations taken at the beginning and end of the campaign, so pipeline data products were typically available one to several weeks after the end of an instrument campaign. The goal was to have the data available to the observer two weeks after the end of the campaign. This was usually the case for IRAC and MIPS; IRS took longer.

The SSC validated the pipeline processing for each observing mode prior to the first release of data. A basic quality assessment was performed on all Spitzer data before they are delivered to the archive. Quality assessment information is also available to the user through the Spitzer Heritage Archive interface.

4.3 Astronomical Observation Templates – AOTs

The observer's interface to the observatory, including the science instruments, was the Astronomical Observation Template (AOT). Spitzer's science instruments are relatively simple in the sense of having few modes and even fewer moving parts (only two - the MIPS scan mirror and the IRAC shutter (see the Instrument Handbooks for more information). The use of relatively simple parameterized observing modes enhanced the reliability of observations and calibration, improved the archival value of Spitzer data, and reduced cost. An AOT was a specific observing mode. In the cryogenic mission there were nine AOTs for the three science instruments. Five of the AOTs (IRAC Mapping, IRS Staring, IRS Spectral Mapping, MIPS Photometry, and MIPS Scan) were commissioned during the first three months following launch. Another AOT (MIPS Spectral Energy Distribution [SED] mode) was available for the Cycle-1 Call for Proposals, though observations were not scheduled until the AOT was commissioned in October 2004. Two AOTs became available, beginning in Cycle-2: MIPS Total Power [TP] mode, and IRS Peak-Up Imaging (PUI). For the warm mission one AOT was commissioned in July 2009: the IRAC Post-Cryo Mapping. The observing modes are:

InfraRed Array Camera (IRAC) Mapping/Photometry

The IRAC AOT is used for simultaneous imaging at 3.6, 4.5, 5.8 and 8.0 microns, over the two ~5.2' x ~5.2' fields of view. This AOT was used for IRAC observations in the cryogenic mission.

InfraRed Array Camera (IRAC) Post-Cryo Mapping/Photometry

The IRAC AOT is used for warm mission observations. It has simultaneous imaging at 3.6 and 4.5 microns, over the two ~5.2' x ~5.2' fields of view. The 5.8 and 8.0 micron arrays were not operational in the warm mission. In September of 2011 peak-up functionality was added to this AOT to assist with high precision time series photometry.

InfraRed Spectrograph (IRS) Staring-Mode Spectroscopy

The IRS staring mode is used for low-resolution long-slit spectroscopy (R= 64–128) from 5.2 to 38.0 microns and high-resolution spectroscopy (R~600) from 9.9 to 37.2 microns. The IRS Staring mode also supports raster mapping. It also returns images from the IRS Peak-Up array, which has a field-of-view of 1' x 1.2' and two filters covering 13.5–18.5 microns and 18.5–26 microns.

IRS Spectral Mapping

The IRS Spectral Mapping AOT is used to perform slit scanning spectroscopy for fields up to a few arcminutes in extent.

IRS Peak-Up Imaging

The IRS Peak-Up Imaging AOT provides imaging only using the Peak-Up array, which has a field-of-view of 1' x 1.2' and two filters covering 13.5–18.5 microns and 18.5–26 microns.

Multiband Imaging Photometer for Spitzer (MIPS) Photometry and Super Resolution Imaging

The MIPS Photometry and Super Resolution AOT is used for imaging photometry and high-resolution imaging at 24, 70 and 160 microns. An "enhanced" small-field mode for 160 microns observations is also available.

MIPS Scan Mapping

The MIPS Scan Map AOT is used for large field maps at 24, 70 and 160 microns. The maps are constructed using slow telescope scanning, combined with motion compensation using a cryogenic scan mirror. Maps are built up of ~5 arcminutes (2.5 arcminutes for full coverage at 70 microns) wide strips between 0.5° and 6° in length.

MIPS Spectral Energy Distribution (SED)

The MIPS Spectral Energy Distribution AOT is used for very low-resolution (R=15–25) spectroscopy covering 52-97 microns using the MIPS 70 micron Ge:Ga array.

MIPS Total Power Measurement (TP)

The MIPS Total Power Mode AOT provides zero-level-reference observations for absolute brightness of extended sources.

Each AOT and its usage are discussed in detail within the respective Instrument Handbooks.

4.4 Astronomical Observation Request – AOR

When all the relevant parameters for an AOT are specified and linked to a description of the target, the resulting fully specified observation is called an AOR, which is the fundamental unit of Spitzer observing. An AOR can be thought of as a list of parameters that, when properly interpreted, completely describe an observation. In fact, an AOR, as represented in the SODB, contained a series of keywords and values that were used to create the sequence of commands that are sent to the observatory to carry out the observation.

An AOR could not be subdivided, could not be interrupted for other activities (such as downlinks), and was handled as a unit by the observatory. Because of this non-interruptible nature and the need to perform certain activities periodically (e.g., detector anneals, pointing system calibrations, and downlinks) a maximum duration existed for an AOR. Originally all AORs had a maximum duration of three hours. As the prime mission progressed the excellent performance of the instruments and the observatory allowed the maximum duration to be extended to 8 hours for IRS and 24 hours for IRAC AORs. The maximum duration of MIPS

AORs was extended to six hours but it was reduced back to three hours when it was determined that germanium anneals every three hours really did produce the best calibrated data. Longer observations could be specified using multiple AORs and relational constraints to identify these AORs as members of a related group.

An AOR contains three categories of information:

Astronomical Target
The target of an AOR can be a single pointing or a cluster of pointings within a 1º radius, at which the specified observation is repeated identically. The single pointing or cluster may be either of an inertial target or a moving target.

AOT-Specific Parameters
As the name implies, these vary from AOT to AOT. They include instrument configuration, exposure time and dedicated mapping parameters.

Timing and Relational Constraints
These constraints represent scheduling directives for an AOR or for a related group of AORs. The details of the kind of constraints that are supported are in section 4.2.1.5. Timing constraints are used to specify a window when an AOR should be executed (e.g., to observe a comet at maximum solar elongation). Relational constraints are used to specify how AORs within a group are related to one another (e.g., a series of AORs that define a very deep map and must be executed consecutively).

4.5 Science User Tools

Science User Tools are software packages and other materials (such as tables and graphs) that are provided by SSC to help the astronomical community plan, prepare, submit, monitor, and interpret the results of their Spitzer observations. They are all available from the IRSA Web site https://irsa.ipac.caltech.edu/data/SPITZER/docs/. We highlight a few tools here for illustrative purposes.

4.5.1 Spot

Spot was a multi-platform Java-based, client-server, GUI-driven software tool intended to assist potential and approved observers in planning and modifying their observations. It allowed investigators to construct and edit detailed AORs by entering targets and selecting from a variety of preset instrument-specific functions (e.g., exposure times, instrument modes, dither patterns, and observing constraints). Spot also included useful visualization tools to permit an investigator to see how proposed observations and the Spitzer focal plane is laid out on the celestial sky. These capabilities allowed observers to retrieve relevant images from other astronomical surveys (in any of a number of wavelengths) and archives. It calculated estimates of Spitzer observing time (including telescope overheads) for each AOR in a proposed program, along with target visibility information, focal plane position angle for a selected observation date, and estimates of the zodiacal and cosmic infrared background at the target. Spot also allowed investigators to view AORs from all previously approved programs.

Spot required a network connection to the Spitzer Science Center servers to obtain observing time estimates, visibility, orientation, or background estimate information, and to submit and update

proposals. A network connection was not necessary for selecting observation parameters. Spot is no longer available for download and is no longer supported.

4.5.2 Performance Estimation Tool (PET)

The most important website-based SSC tool is the Performance Estimation Tool (PET). The PET is actually a set of JavaScript tools to aid in designing Spitzer observations. There are four PET components: The Sensitivity PET, the Spectroscopy PET, the Extragalactic PET, and the Stellar PET. Users of the PET should pay close attention to the various notes and warnings on both the main PET pages and the help pages.

The Sensitivity PET (SENS-PET) is an imaging sensitivity estimator. It takes as input IRAC, IRS PUI, and/or MIPS imaging instrument configurations, and a background level. It produces as output the instrument sensitivities (both for point source and extended objects), and the total exposure depth per pixel.

The Spectroscopy PET (SPEC-PET) is designed specifically for spectroscopic sensitivity estimates. Users configure IRS and/or MIPS SED observing parameters, and the SPEC-PET returns an estimate of the instrument sensitivity.

The Extragalactic PET (EX-PET) makes predictions for imaging of extragalactic sources. As input, users may choose an SED model, background level, and IRAC + MIPS instrument configurations. The output includes flux in the instrument passbands, instrument sensitivities, S/N, and total exposure depth per pixel.

Finally, the Stellar PET (STAR-PET) predicts fluxes for imaging of stars. For input, users select a stellar spectral type + MK class, K-band magnitude or K-band flux density. The tool calculates the expected flux density in the IRAC 3.6, 4.5, 5.8, 8.0 microns passbands, and at 15 microns (IRS peak-up blue channel and short wavelength module), and 24 microns (IRS peak-up red channel and long wavelength module, and MIPS Si:As array).

You can find the PETs at
https://irsa.ipac.caltech.edu/data/SPITZER/docs/dataanalysistools/tools/pet/

4.5.3 Spitzer Heritage Archive

The first observer's interface to the archive was called Leopard (delivered within the Spitzer-Pride package of Observation Planning software), and was very similar to Spot (see above). In November 2009 the Spitzer Heritage Archive (SHA), a web-based interface, began to also serve proprietary Spitzer data and became *the* Spitzer Archive. Information about how to retrieve public and/or proprietary data using the SHA can be found at the SHA URL:
http://sha.ipac.caltech.edu/applications/Spitzer/SHA .

4.6 Solar System Objects - SSOs

Spitzer supported observations of Solar System objects, tracking in linear segments at rates up to 1 arcsecond/second. All instruments and all observing modes could be used while tracking.

During IOC/SV, IRS peak-up for IRS spectroscopy was successful for all moving targets attempted, which included objects with rates between <1.0 arcseconds/hour and just over 200 arcseconds/hour, and fluxes between 40 mJy and 1 Jy at 15 microns. Peak-up on both point source and extended targets were supported; during IOC/SV, both moving point sources and extended sources were acquired. However, note that peak-ups were not restricted to be performed only on the moving target being tracked, or a point source that is co-moving with it; instead, observers could peak up on an inertial target and then offset to a moving target.

4.6.1 Tracking Performance

Spitzer's SSO tracking capability is similar to its scanning capability. One significant consequence of this for the Solar System observer involves sources whose tracks, on an equatorial map, have significant curvature during an AOR. Such AORs may have needed to be broken up into a series of short (linear) AORs. The spacecraft does not carry any target ephemerides on board, so the track was defined at the time of scheduling and formulated as a vector rate in an equatorial frame. A start time and equatorial J2000 start point and time were also provided for use by the PCS. Once the track command has been issued, the on-board system maintained knowledge of where the telescope should be at what time, and "catches up" with the specified track and maintains it.

4.6.2 Ephemeris Management

Spitzer used a database of ephemerides for known SSOs derived from the Horizons database maintained by the Solar System Dynamics group at the Jet Propulsion Laboratory. For proposal planning purposes, Spot could retrieve the ephemerides for a specified target by resolving the NAIF ID. These ephemerides were used to calculate visibility windows and resource estimate calculations for SSOs through Spot.

4.6.2.1 Shadow Observations

The infrared flux from background sources, and particularly small-scale structure in that background, frequently limits the sensitivity of Spitzer, particularly in the wavelength range 24–160 microns. To assist in background subtraction, Solar System observers could specify "shadow" background observations for all instruments and observing modes. A shadow observation allowed the track across the sky taken during observation of a moving target to be replayed or pre-played when the target is not there. Shadow observations allow the Solar System observer to remove background small-scale structure, thereby improving moving target sensitivity. To reduce potential errors due to time-dependent changes in the zodiacal light, instrument characteristics, and calibration, a shadow observation is generally most effective when taken as close in time to the primary observation as is scientifically possible. Execution of the shadow observation *after* observation of the science target was the default (much easier to schedule both observations), although there are situations where this is not the optimal executing order.

4.7 Targets of Opportunity - ToOs

Targets of Opportunity are transient events whose timing is unpredictable. Predictable phenomena whose precise timing is not known a priori (e.g., novae, newly discovered comets, gamma-ray bursts) may have been requested in a General Observer proposal (i.e. within a normal Call for Proposals). Observations of completely unanticipated phenomena could be requested through Director's Discretionary Time proposals.

ToOs were classified based solely on their impact on the observatory scheduling process, which depends on the time elapsed between the activation of a ToO observing request and the desired date of execution of the corresponding observation; see Table 4.1 for ToO classification criteria.

Table 4.1: Classification of ToOs

High impact	<1 week (48 hour minimum turnaround)
Medium impact	1–5 weeks (1-8 weeks in warm mission)
Low impact	>5 weeks (>8 weeks in warm mission)

4.8 Generic Targets

Generic Targets can be scientifically described, but do not have exact celestial coordinates or brightness estimates at the time of proposal submission. An example of this would be objects discovered in a survey (by Spitzer or any other telescope) for which IRS spectroscopy is sought. Integration time estimates within a factor of 1.5 must have been provided in the generic target AOR and a position within 2° of the expected final position.

4.9 Second-Look Observations

Second-look observations (SLOs) were deemed to be a predictable element of an integrated Spitzer observing program, even if the specific targets cannot be provided at the time of proposal submission. For example, an investigator could propose for 80 hours of time to conduct one-hour observations of 30 targets and then ten-hour observations of the five most interesting of these based on criteria spelled out in the proposal. Because of the expected end of cryogen in Cycle-5 SLOs were not allowed as part of Cycle-5 programs. Second look observations were allowed in the warm mission.

4.10 List of Safings or Standbys in the Mission

There were 13 safe modes or standbys during normal science observations in the mission. Several were due to single events (i.e. a proton hit) that caused a piece of hardware (i.e. the CE or the IRU) to produce an error and the fault protection requested a standby or safe mode as it was designed to do. The events are listed in the order in which they occurred. The "Days Back to Science" column lists the number of days (rounded to the nearest whole day) before science

observations were resumed. Within the 18 August 2006 safe mode there was another event on 28 August (false OPZ violation by the WASS) before science observations had been re-started.

Table 4.2: List of Safe/Standby modes during normal science operations

Entry Date UT	Safe/ Standby	Instrument On	Days Back to Science	Event
11 December 2003	Standby	MIPS	2	CE FIFO error counter
30 December 2003	SafeMode	MIPS	4	Reaction wheel stiction
25 January 2004	Standby	MIPS	1	CE unprotected global variables
5 February 2004	Standby	IRS	1	CE spurious interrupt
10 June 2004	SafeMode	IRAC	7	IRU false indication of OPZ violation
24 April 2005	SafeMode	IRS	11	IRU stuck relay
9 May 2006	SafeMode	MIPS	2	Star-tracker data corrupted
18 August 2006	SafeMode	MIPS	13	Observatory side swap (on side B from this point)
27 March 2008	Standby	IRS	9	CE corrupted IRS data
28 February 2009	Standby	IRS	4	CE multi-bit error
15 May 2009	Standby	IRAC	N/A	End of cryogen
27 November 2015	Standby	IRAC	17	IRAC/SC Communication Anomaly
30 January 2020	SafeMode	None	N/A	End of Mission – commanded from the ground

Chapter 5. Spitzer Cross-Calibration

Spitzer observers and archival researchers will undoubtedly wish to plot measurements from multiple instruments on the same flux scale. While the calibration strategy for each instrument was derived independently (see the Instrument Handbooks for details), checks of the consistency of the absolute calibrations were coordinated by the SSC. The requirement was that the absolute calibrations be consistent to within 10%.

5.1 Observations

A separate cross-calibration observing program was not implemented for Spitzer. Instead, the individual instrument's calibration programs included targets common to two or three instruments. These targets included both dedicated cross-calibrators, and objects selected from the individual teams' lists. Cross- calibration observations were carried out during IOC/SV, and every month or two during nominal operations.

Sensitivity and saturation limits are critical constraints in the choice of cross-calibrator targets. Many traditional infrared calibrators were too bright for Spitzer instruments. For example, Alpha Boo was too bright for all bands except MIPS 160 microns. Planets and the best-understood asteroids are generally even brighter.

5.2 Stellar Cross-Calibrators

Dedicated stellar cross-calibrators were selected in the Continuous Viewing Zone (CVZ). The steeply-falling SEDs of most stellar photospheres in the infrared make it difficult to use just one type of star for cross-calibration. Hence, the stellar cross-calibrators were roughly divided into IRAC/IRS cross-calibrators and IRS/MIPS cross-calibrators.

The stars were chosen from the Hipparcos catalog. Stars of three spectral types were selected: A dwarfs, K giants, and solar-type stars. The K magnitudes of the stars range from about 4 for the K giants to 7 for the A dwarfs and G stars. In addition to these dedicated cross-calibrators, still fainter stars from the IRAC team's list were used for IRAC/IRS cross-calibration. Additional stars common to both IRS and MIPS, but not in the CVZ, were also used.

5.3 Red Cross-Calibrators

The absolute calibrations of all three instruments are mainly based on stars. Since the stars are blue in the infrared, cross-calibrators with much redder spectral energy distributions were observed as an additional check not covered by the stellar cross-calibrators.

Since planets and well-known asteroids were too bright for most Spitzer bands, galaxies with few infrared spectral features have been selected as red cross-calibrators for IRAC and MIPS. Type-1 (radio-quiet) AGNs lack strong features in the IRAC, IRS, and MIPS 24 micron bandpasses.

Galaxies with a 24 micron flux density of a few hundred mJy were suitable. Mrk 279 and IRAS 23060+0505 were among the galaxies being observed for this purpose.

Table 5.1: IOC/SV cross-calibration targets.

Name	**Observed by...**
Mrk 279	IRS, MIPS
HD 176841	IRS, MIPS
HD 180711 (HR 7310)	IRS, MIPS
KF01T4	IRAC, IRS
KF03T2	IRAC, IRS
HD 170693	IRS, MIPS
HD 173398	IRS, MIPS
HD 172728 (HR 7018)	IRAC, IRS, MIPS
HD 173511	IRAC, IRS, MIPS
HD 154391 (HR 6348)	IRAC, IRS, MIPS
BD +60D1753	IRAC, IRS
HD 238928	IRAC, IRS
HD 165459	IRAC, MIPS
HD 166780	IRAC, IRS, MIPS
HD 159330 (HR 6540)	IRAC, IRS, MIPS
HD 163588 (ksi Dra, HR 6688)	IRS, MIPS
HD 82621 (26 UMa)	IRS, MIPS
HD 164058 (Gam Dra, HR 6705)	IRS, MIPS
HD 89758 (mu UMa)	IRS, MIPS
HD 62059 (Beta Gem)	IRS, MIPS
HD 48915 (HR 2491, alpha CMa)	IRS, MIPS
HD 39608	IRS, MIPS
HD 41371	IRS, MIPS
HD 42701	IRS, MIPS

Chapter 6. Spitzer Archive

This section describes the basic data products the user will receive from the Spitzer Archive.

The data delivery consists of a directory hierarchy with a name unique to that AOR. In this hierarchy are the Level 1 (Basic Calibrated Data, BCD), as well as a number of subdirectories containing the Level 0 (raw data), the calibration files, log files, and the Level 2 (post-BCD) data. The exact contents of the data delivery vary according to what the user has requested from the Spitzer Heritage Archive.

The FITS headers are populated with keywords including (but not limited to) physical sky coordinates and dimensions, a photometric solution, details of the instrument and spacecraft including telemetry when the data were taken, and the steps taken during pipeline processing. There are three primary image data types that are supplied for each AOR (raw, BCD, post-BCD).

6.1 Level 0, or Raw Data

Raw data are wholly unprocessed, except for those steps necessary to render them into a readable FITS format, i.e., depacketization and decompression. They are, however, supplied in the event that users wish to reprocess their data in a different manner from the pipeline processing. By comparison to ground-based astronomy, these are the raw data one gets from a camera and writes to disk while observing at the telescope.

6.2 Level 1, or Basic Calibrated Data (BCD)

BCDs are exposure-level data after having passed through the pipelines. Instrumental signatures have been mostly removed, and the BCDs have been absolutely calibrated into physical units (i.e., MJy/sr = 10^{-17} erg s^{-1} cm^{-2} Hz^{-1} sr^{-1}). Continuing the analogy with ground-based observing, the BCDs are data that have been reduced, but not yet combined into a final image. This is the primary science data product that was produced by the SSC.

Ancillary files are supplied with each BCD. These ancillary files contain several types of information regarding each pixel in each image. An image containing the uncertainty for each pixel is supplied. A mask image contains status bits indicating the probability that any given pixel has been affected by adversely by a known effect. Log files are also supplied, and from these and the header keywords the entire pedigree of every data product can be derived.

All of the data and ancillary files are in FITS format, containing a header with keywords and their values followed by a binary image, except certain log files that are in simple ASCII format. The standard FITS header keywords are all present, so that essentially any FITS file reader is able to read the files.

6.3 Calibration Files

For each BCD, the pipeline calibration server generated several estimates of the current detector characteristics. These calibration files are supplied to the user. Users are also able to request from the Archive the files that were used to generate, e.g., the sky darks, sky flats, and absolute calibration. The photometric calibrators are not included with each science observation, but they are available via a separate request to the Archive.

6.4 Level 2, or Extended Pipeline Products (Post-BCD)

Pipeline processing of Spitzer data by the SSC also included more advanced processing of many individual data frames together to form more "reduced" data products. Known by the generic title of "post-BCD" processing, this extended pipeline refined the telescope pointing, produces mosaicked images and combined spectra.

6.5 Calibrated Data Units

The BCD product, which is the primary data provided to users after pipeline processing, consists of individual frames where the pixel values are in units of MJy/sr. Jansky is a flux density unit defined as:

$$1 \text{ Jansky} = 1 \text{ Jy} = 10^{-26} \text{ W m}^{-2} \text{ Hz}^{-1} = F_\nu \quad (6.1)$$

The conversion between Jansky and flux density in W m^{-2} per unit wavelength is accomplished via

$$F_\nu \times 10^{-26} \times c/\lambda^2 = F_\lambda \quad (6.2)$$

where the wavelength bin-width is specified in the same length units as λ and c. For example, if c is taken as 3×10^{14} μm s^{-1} and λ is specified in microns, the above equation results in F_ν being in units of W m^{-2} μm^{-1}.

Appendix A. Infrared Astronomy

Infrared Flux Units

The infrared flux density from a point source is most commonly given in units of Jansky (Jy) where:

1 Jy = 10^{-23} erg s^{-1} cm^{-2} Hz^{-1} = 10^{-26} Watts m^{-2} Hz^{-1} = F_ν

The conversion between Janskys and flux density in Wm^{-2} per unit wavelength is given by:

$F_\nu x\ 10^{-26}\ x\ c/\lambda^2 = F_\lambda$

The infrared flux density from an area on the sky, such as the surface brightness of an extended object, or the background emission, is commonly given in 10^6 Jy steradian^{-1} = 1 MJy sr^{-1}. Another common unit is Jy per square arcsecond; 1 MJy sr^{-1} = 2.350443 × 10^{-5} Jy $arcsec^{-2}$.

Tables A1- A3 list the zero magnitude fluxes for various common optical and infrared filters. Note that the photometric system of filter sets can vary, depending on the manufacturer. The magnitude of a source can be converted to a flux density using:

$F_\nu = F_0 \times 10^{(-m/2.5)}$

There is an online Javascript tool available from the IRSA Web site that interactively converts Janskys to magnitudes (or any of a variety of flux units) and vice versa. You can find it at https://irsa.ipac.caltech.edu/data/SPITZER/docs/dataanalysistools/tools/pet/magtojy/

Table A 1: 2MASS system zero points

Passband	Effective wavelength (microns)	Zero point (Jy)
J	1.235	1594
H	1.662	1024
Ks	2.159	666.7

References: Table 2 from Cohen, Wheaton, & Megeath 2003, AJ, 126, 1090; see also 2MASS All-Sky data release document: http://www.ipac.caltech.edu/2mass/releases/allsky/doc/explsup.html

Table A 2: Johnson system zero points

Passband	Effective wavelength (microns)	Zero point (Jy)
U	0.36	1823
B	0.44	4130
V	0.55	3781
R	0.71	2941
I	0.97	2635

Passband	Effective wavelength (microns)	Zero point (Jy)
J	1.25	1603
H	1.60	1075
K	2.22	667
L	3.54	288
M	4.80	170
N	10.6	36
O	21.0	9.4

References: *Allen's Astrophysical Quantities*, Fourth edition, 2001, Arthur N. Cox (ed.), Springer-Verlag; Campins, Rieke, & Lebofsky 1985, AJ, 90, 896; Rieke, Lebofsky, & Low 1985, AJ, 90, 900.

Table A 3: UKIRT system zero points

Passband	Effective wavelength (microns)	Zeropoint (Jy)
V	0.5556	3540
I	0.9	2250
J	1.25	1600
H	1.65	1020
K	2.20	657
L	3.45	290
L'	3.80	252
M	4.8	163
N	10.1	39.8
Q	20.0	10.4

References: UKIRT Web page:
https://www.ukirt.hawaii.edu/astronomy/calib/phot_cal/conver.html

Infrared Backgrounds

Various astronomical sources emit radiation in the infrared part of the spectrum. Cool stars (M class) have their peak emission just short of the near infrared. However, stars with dusty envelopes or shells and circumstellar disks can be quite bright in the infrared. Regions of star formation, HII regions, and planetary nebulae are strong infrared sources. The (relatively) cool interstellar medium in galaxies has an infrared component. There are also ultra-luminous infrared bright galaxies that are very strong sources of infrared radiation.

As in the optical, the infrared zody is concentrated toward the ecliptic with weaker emission, by approximately a factor of 4, toward the ecliptic poles. The infrared zody is strongest from about 5 microns to about 30 microns with peak emission at about 10 microns. The infrared zody has structure on most scales and, as observed from Earth, varies from season to season. The intensity of the infrared zody will also vary with solar elongation, or how close to the Sun one is pointed. The infrared zody is difficult to model.

As one moves to longer wavelengths (100 microns), diffuse Galactic emission from dust clouds in the interstellar medium becomes the dominant contribution to the infrared background. This infrared cirrus is patchy, with higher concentrations found in the Galactic disk and toward the

Galactic center. However, it is important to realize that the cirrus is ubiquitous, and it is critical to examine the IRAS maps or radio maps of cirrus tracers when planning longer-wavelength observing. Far-infrared emission from external galaxies in the field of view will add to the overall background flux.

Solar System Objects Included in Bright Object Avoidance

Earth
Moon
Mars
Jupiter
Saturn
Uranus
Neptune
4 Vesta
6 Hebe
1 Ceres
7 Iris
15 Eunomia

Appendix B. Acronyms and Glossary

The following lists the acronyms used in this manual.

2MASS	2 Micron All Sky Survey
AOR	Astronomical Observation Request(s)
AOT	Astronomical Observation Template(s)
BCD	Basic Calibrated Data
BIC	Baseline Instrument Campaign Plan
C&DH	Command and Data Handling
CA	Cryogenic Assembly
CE	Combined Electronics
CP	Call for Proposals
CTA	Cryogenic Telescope Assembly
CTIA	Capacitive TransImpedence Amplifier
CVZ	Continuous Viewing Zone
DDT	Director's Discretionary Time
Dec	Declination
DSN	Deep Space Network
FAQ	Frequently Asked Question
FITS	Flexible Image Transport System
FLS	First Look Survey
FOV	Field-of-View
GO	General Observers
GTO	Guaranteed Time Observer(s)
HGA	High Gain Antenna
IBC	Impurity Band Conduction
ICRS	International Celestial Reference System
IER	Instrument Engineering Request – like an AOR, but for specific engineering tasks not able to be accomplished using an AOR.
IOC	In-Orbit Check out
IPAC	Infrared Processing and Analysis Center
IR	Infrared
IRAC	InfraRed Array Camera
IRAS	InfraRed Astronomical Satellite
IRS	InfraRed Spectrograph
IRSA	Infrared Science Archive
IRU	Inertial Reference Unit
ISO	Infrared Space Observatory
ISSA	IRAS Sky Survey Atlas
IWIC	IRAC Warm Instrument Characterization
JPL	Jet Propulsion Laboratory
Jy	Jansky
LGA	Low Gain Antennae
MIC	Multi-Instrument Chamber
MIPS	Multiband Imaging Photometer for Spitzer
mJy	milliJansky
MJy	megaJansky
MPC	Minor Planet Center

OPZ	Operational Pointing Zone
PAO	Period of Autonomous Operations
PCRS	Pointing Control Reference Sensor
PCS	Pointing & Control System
PI	Principal Investigator
PIN	Positive Intrinsic Negative (Diode)
PM	Primary Mirror
PST	Point Source Transmission
PUI	Peak-Up Imaging
RA	Right Ascension
RAM	Random Access Memory
RCS	Reaction Control System
rms	Root Mean Square
ROC	Reserved Observations Catalog
S/C	SpaceCraft
SED	Spectral Energy Distribution
SHA	Spitzer Heritage Archive
SIRTF	Space InfraRed Telescope Facility, Spitzer's old name
SLO	Second-Look Observation
SM	Secondary Mirror
SODB	Science Operations Database
SOM	Spitzer Observer's Manual
S/N	Signal to Noise
Spot	Previously listed here as an acronym meaning "Spitzer Planning Observations Tool" but now it is simply a proper noun
sr	Steradians
SSC	Spitzer Science Center
SSC website	Originally http://ssc.spitzer.caltech.edu/ this website has been moved to https://irsa.ipac.caltech.edu/data/SPITZER/docs/
SSO	Solar System Objects/Observations
ST	Star Tracker
ST/IRU	Star Tracker/Inertial Reference Unit
SV	Science Verification
SWG	Science Working Group
TAC	Time Allocation Committee
ToO	Target of Opportunity
TP, TPM	Total Power Mode
WASS	Wide Angle Sun Sensor

Appendix C. Acknowledgments

The success of the Spitzer Space Telescope reflects the talent and dedication of thousands of people who have worked on this project over the past two decades and more, and here they are recognized for their contribution to this success. Many of these people, by the institutions through which they participated, shaped the definition, development, and/or operations of Spitzer. We hope that this recognition provides a tangible though modest token of our gratitude and that they—and others whom we may have inadvertently omitted from the lists—are able to share with us the excitement of the fruits of our collective labors.

SIRTF Science Working Group: M. Werner, JPL, Project Scientist; C. Lawrence, JPL, Deputy Project Scientist; T. Roellig, NASA Ames, Facility Scientist; G. Fazio, SAO, IRAC Principal Investigator; J. Houck, Cornell, Principal Investigator; G. Rieke, U. Arizona, MIPS Principal Investigator; D. Cruikshank, NASA Ames; R. Gehrz, U. Minnesota; M. Jura, UCLA; F. Low, U. Arizona; M. Rieke, U. Arizona; B. Thomas Soifer, Caltech, E. Wright, UCLA.

Ball Aerospace (Cryogenic Telescope Assembly): R. Abbott, D. Adams, S. Adams, J. Austin, B. Bailey, H. Bareiss, J. Barnwell, T. Beck, B. Benedict, M. Bilkey, W. Blalock, M. Breth, R. Brown, D. Brunner, D. Burg, W. Burmester, S. Burns, M. Cannon, W. Cash, T. Castetter, M. Cawley, W. Cebula, D. Chaney, G. J. Chodil, C. Cliff, S. Conley, A. Cooper, J. Cornwell Sr., L. Cortelyou, J. Craner, K. Craven, D. Curtis, F. Davis, J, Davis, C. Dayton, M. Denaro, A. DiFronzo, T. Dilworth, N. Dobbins, C. Downey, A. Dreher, R. Drewlow, B. Dubrovin, J. Duncan, D. Durbin, S. Engles, P. Finley, J. Fleming, S. Forrest, R. Fredo, K. Gause, M. Gee, S. Ghesquiere, R. Gifford, J. Good, M. Hanna, D. Happs, F. Hausle, G. Helling, D. Herhager, B. Heurich, E. Hicks, M. Hindman, R. Hopkins, H. Hoshiko Jr., J. Houlton, J. Hueser, J. Hurt, W. Hyatt, K. Jackson, D. Johnson, G. Johnson, P. Johnson, T. Kelly, B. Kelsic, S. Kemper, R. Killmon, R. Knewtson, T. Konetski, B. Kramer, R. Kramer, L. Krauze, T. Laing, R. LaPointe, J. Lee, D. Lemon, P. Lien, R. Lytle, L. Madayev, M. Mann, R. Manning, J. Manriquez, M. Martella, G. Martinez, T. McClure, C. Meier, B. Messervy, K. Modafferi, S. Murray, J. Necas Jr., M. Neitenbach, P. Neuroth, S. Nieczkoski, G. Niswender, E. Norman-Gravseth, R. Oonk, L. Oystol, J. Pace, K. Parrish, A. Pearl Jr., R. Pederson, S. Phanekham, C. Priday, B. Queen, P. Quigley, S. Rearden, M. Reavis, M. Rice, M. Richardson, P. Robinson, C. Rowland, K. Russell, W. Schade, R. Schildgen, C. Schroeder, G. Schultz, R. Schweickart, J. Schweinsberg, J. Schwenker, S. Scott, W. Seelig, L. Seide, K. Shelley, T. Shelton, J. Shykula, J. Sietz, J. Simbai, L. Smeins, K. Sniff, B. Snyder, B. Spath, D. Sterling, N. Stoffer, B. Stone, M. Taylor, R. Taylor, D. Tennant, R. Tio, P. True II, A. Urbach, S. Vallejo, K. Van Leuven, L. Vernon, S. Volz, V. VonRuden, D. Waldeck, J. Wassmer, B. Welch, A. Wells, J. Wells, T. Westegard, C. Williamson, E. Worner Jr.,T. Yarnell, J. Yochum, A. Youmans, J. Zynsky.

Cornell University (Infrared Spectrograph): **Cornell (project management and science)**: D. Barry, S. V. W. Beckwith, J. Bernhard-Salas, C. Blacken, B. Brandl, V. Charmandaris, M. Colonno, S. Corbin, P. Devine, D. Devost, J. Diller, K. Duclos, E. Furlan, G. Gull, P. Hall, L. Hao, C. Henderson, T. Herter, J. Higdon, S. Higdon, P. Howell, L. McCall, A. Parks, B. Pirger, A. Rakowski, S. Reinehart, A. Reza, E. E. Salpeter, J. Schoenwald, G. Sloan, J. Smith, H. Spoon, K. Uchida, D. Weedman, J. Wilson; **University of Rochester**: D. M. Watson, W. F. Forrest; **California Institute of Technology**: K. Matthews; **Ball Aerospace (instrument development)**: D. Alderman, D. Anthony, M. Bangert, J. Barnwell, A. Bartels, S. Becker, W. Belcher, J. Bergstrom, D. Bickel, M. Bolton, S. Burcar, D. Burg, S. Burns, S. Burns, D. Burr, P. Burrowes, W. Cebula, C. Conger, J. Crispin, M. Dean, M. D'Ordine, S. Downey, R. Drewlow, L. Duchow, D. Eva, C. Evans, M. Foster, S. Fujita, D. Gallagher, A. Gaspers, P. Gentry, S. Giddens, J. Graw,

M. Hanna, A. Haralson, M. Henderson, D. Herhager, J. Hill, S. Horacek, M. Huisjen, S. Hunter, J. Jacob, R. Karre, L. Larsen, P. Lien, R. Manning, J. Marriott, D. McConnell, R. McIntosh, M. McIntosh, G. Mead, B. Michelson, B. Miller, J. Moorehead, M. Morris, J. Murphy, M. Nelson, J. Pacha, I. Patrick, A. Pearl, B. Pett, S. Randall, C. Rowland, R. Sandoval, D. Sealman, K. Shelley, J. Simbai, L. Smeins, C. Stewart, G. Taudien, D. Tennant, J. Troeltzsch, B. Unruh, J. van Cleve, C. Varner, J. Winghart, J. Workman; **Rockwell (detector arrays)**: B. Beardwood, J. Huffman, D. Reynolds, D. Seib, M. Stapelbroek, S. Stetson; **OCLI (filters)**: S. Corda, B. Dungan, D. Favot, S. Highland, M. Inong, V. Jauregui, C. Kennemore, B. Langley, S. Mansour, R. Mapes, M. Mazzuchi, C. Piazzo.

Jet Propulsion Laboratory, California Institute of Technology (project and science management, mission operations): D. Achhnani, A. Agrawal, T. Alfery, S. Ancheta, K. Anderson, J. Arnett, B. Arroyo, D. Avila, W. Barboza, M. Bareh, S. Barry, D. Bayard, C. Beichman, M. Beltran, R. Bennett, P. Beyer, K. Bezjak, K. Bilby, D. Bliss, G. Bonfiglio, M. Bothwell, J. Bottenfield, D. Boussalis, E. Boyd, C. Boyles, J. Brickman, M. Brown, P. Brugarolas, E. Buck, R. Bunker, C. Cagle, P. Candelaria, C. Carrion, J. Casani, E. Cherniack , E. Clark, C. Cofield, D. Cole, J. Craft, J. Cruz, M. Deutsch, S. Dodd, J. Dooley, S. Dekany, R. Dumas, M. Ebersole, P. Eisenhardt, C. Elachi, W. Ellery, D. Elliott, M. Epstein, K. Erickson, D. Espitallier, J. Evans, W. Evenson, P. Falkenstern, J. Fanson, T. Feehan, A. Forinash, R. Fragoso, L. Francis, R. Franco, D. Gallagher, M. Gallagher, G. Ganapathi, M. Garcia, N. Gautier, T. Gavin, S. Giacoma, J. Gilbert, L. Gilliam, C. Glazer, P. Gluck, M. Goman, V. Gorjian, G. Greanias, M. Griffin, C. Guernsey, A. Guerrero, P. Haas, M. Hashemi, G. Havens, C. Hegedus, C. Hidalgo, E. Higa, G. Hill, J. Hodder, H. Hotz, W. Hu, L. Huerta, N. Hughes, J. Hunt Jr., D. Hurley, J. Ibanez, W. Irace, K. Jin, M. Johansen, M. Jones, B. Kahr, J. Kahr, B. Kang, P. Kaskiewicz, J. Keene, D. Kern, T. Kia, M. Kline, B. Korechoff, P. Kwan, J. Kwok, H. Kwong-Fu, E. Landau, M. Larson, C. Leeds, M. Leeds, R. Lineaweaver, S. Linick, P. Lock, W. Lombard, S. Long, T. Luchik, J. Lumsden, M. Lysek, G. Macala, S. Macenka, P. MacMillin, A. Mainzer, N. Mainland, K. Martin, E. Martinez, M. Mcauley, T. McKenzie, J. Mehta, P. Menon, T. Merkley, G. Miller, R. Miller, C. Miyamoto, W. Moore, F. Morales, R. Morris, K. Moua, A. Nakata, B. Naron, A. Nash, D. Nichols, R. Olds, M. Osmolovsky, J. Owen, K. Owen-Mankovich, K. Patel, S. Peer, J. Platt, N. Portugues, D. Potts, S. Ramsey, S. Rangel, C. Regmund, R. Reid, J. Reimer, E. Rice, D. Rockey, E. Romana, C. Rondeau, A. Sanders, S. Sanders, W. Santiago, M. Sarrel, V. Scarffe, T. Scharton, H. Schember C. Scott, J. Schott, P. K. Sharma, T. Shaw, D. Shebel, J. Short, L. Simmons, C. Simon, B. Smith, R. Smith, P. Sorci, T. Specht, R. Spehalski, G. Squibb, S. Stanboli, K. Stapelfeldt, D. Stern, A. Stewart, L. Storrie-Lombardi, K. Stowers, J. Stultz, M. Susak, M. Tankenson, N. Thomas, R. Thomas, F. Tolivar, R. Torkelson, R. Torres, R. Tung, N. Vandermey, P. Varghese, H. Vecchione, M. Viotti, M. Vogt, V. Voskanian, B. Waggoner, L. Wainio, T. Weise, J. Weiss, K. Weld, M. Weller, R. Wilson, M. Winters, S. Wissler, G. Yankura, K. Yetter.

Lockheed-Martin (spacecraft, systems engineering, spacecraft operations): B. Adams, J. Akbarzadeh, K. Aline, T. Alt, S. Ancheta, G. Andersen, J. Arends, F. Arioli, A. Auyeung, D. Bell, R. Bell, F. Bennett, J. Bennett, M. Berning, R. Berry, H. Betts, G. Beutelschies, K. Bezjak, M. Billian, E. Boyd, J. Brickman, S. Broadhead, B. Bocz, G. Bollendonk, N. Bossio, P. Boyle, T. Bridges, C. Brink, R. Brookner, J. Brunton, E. Buck, D. Bucher, J. Burbach, M. Burrack, R. Caffrey, P. Candelaria, S. Carmer, P. Carney, T. Carpenter, R. Castro, J. Cattrysse, J. Cernac, G. Cesarone, K. Chan, C. Chang, M. Chuang, D. Chenette, A. Chopra, Z. Chou, W. Christensen, K. Chu, W. Clark, J. Clayton, S. Cleland, W. Clements, C. Colborn, A. Cooprider, B. Corwin, B. Costanzo, D. Cortes, M. Cox, M. Cox, J. Coyne, J. Crocker, C. Cuddy, S. Curtin, G. Dankiewicz, C. Darr, J. Dates, J. Day, S. DeBrock, T. Decker, R. Defoe, J. Delavan, G. Delezynski, J. Delk, B. Dempsey, R. Dodder, T. Dougherty, H. Drosdat, G. Du, B. Dudginski, M. Dunn, R. Dunn, M.

Dunnam, D. Durant, D. Eckart, B. Edwards, M. Effertz, L. Ellis, P. Emig, M. Epstein, D. Espitallier, N. Etling, M. Etz, W. Evenson, P. Falkenstern, N. Fernando, C. Figge, R. Finch, S. Finnell, A. Fisher, M. Fisher, P. Fleming, D. Ford, A. Forinash, K. Foster, J. Frakes, R. Franco, P. Frankel, D. Fulton, P. Galli, D. Garcia, M. Gardner, B. Garner, S. Gaskin, S. Gasner, T. Gasparrini, M. Geil, E. Georgieva, T. Gibson, B. Goddard, M. Goman, M. Gonzalez, D. Goold, D. Graves, S. Gray, M. Griffin, I. Grimm, J. Grinwis, M. Gronet, R. Grubic, S. Guyer, M. Haggard, J. Harrison, P. Haas, G. Hauser, C. Hayashi, P. Headley, W. Hegarty, C. Hegedus, S. Heires, J. Herrerias, D. Hirsch, K. Hooper, J. Horwath, S. Housten, D. Howell, L. Huerta, L. Huff, N. Hughes, G. Idemoto, B. Jackson, K. Janeiro, K. Johnson, M. Johnson, R. Kaiser, P. Kallemeyn, G. Kang, R. Kasuda, M. Kawasaki, B. Keeney, J. Kenworthy, C. King, A. Klavins, K. Klein, C. Klien, P. Klier, C. Koch, L. Koch, D. Koide, R. Kriegbaum, J. Kuchera, J. Ladewig, D. Lance, M. Lang, K. Lauffer, A. Lee, E. Lee, J. Lee, R. Lee, C. Leeds, D. Leister, K. Loar, A. Lott, C. Love, N. Iyengar, P. Ma, P. MacMillin, A. Magallanes, A. Mainzer, T. Maloney, S. Mar, B. Marquardt, C. Martin, K. Martin, M. Martin, G. Mason, R. Maxwell, R. May, G. McAllister, S. McElheny, M. McGee, J. McGowan, T. McKenzie, D. McKinney, A. McMechen, T. Merkley, E. Merlo, C. Mifsud, J. Miles, G. Miller, S. Miller, A. Minter, C. Miran, S. Mittal, R. Mock, R. Mock, J. Montgomery, J. Moore, H. Mora, M. Moradia, L. Morales, R. Morales, G. Morison, J. Mota, K. Moua, F. Moules, S. Mumaw, L. Naes, A. Nalbandian, J. Nelson, L. Nenoff, J. Neuman, D. Nguyen, K. Nguyen, T. Nguyen, D. Niebur, D. Nishimura, M. Ochs, R. Olds, T. Oliver, J. Oo, J. Ortiz, J. Owen, G. Pace, L. Padgett, N. Page, G. Painter, H. Pandya, L. Pappas, N. Pemberton, R. Peterson, H. Phan, L. Phan, J. Pine, R. Poling, R. Potash, D. Radtke, W. Ramos, T. Ransom, M. Ratajczyk, D. Read, S. Ready, C. Regmund, M. Rich, R. Richey, H. Rizvi, C. Rollin, C. Rudy, M. Rugebregt, R. Russek, B. Sable, S. Sanders, C. Sandwick, W. Santiago, M. Santos, N. Schieler, J. Schirle, G. Schlueter, M. Schmitzer, J. Schott, E. Sedivy, R. Seeders, S. Selover, R. Shaw, F. Sheetz, D. Shelton, R. Sherman, T. Sherrill, O. Short, R. Sison, B. Smith, F. Smith, S. Smith, B. Sotak, S. Spath, J. St. Pierre, K. Starnes, A. Stewart, K. Stowers, J. Straetker, T. Stretch, S. Sulak, W. Sun, M. Susak, D. Swanson, C. Tatro, M. Tebo, D. Telford, A. Tessaro, J. Tietz, D. Tenerelli, J. Tolomeo, R. Torkelson, S. Toro-Allen, J. Tousseau, R. Traber, M. Tran, P. Travis, K. Uselman, S. Utke, N. Vadlamudi, R. VanBezooijen, J. Vantuno, R. Vasquez, H. Vecchione, G. Vergho, C. Voth, B. Vu, P. Wagner, M. Weller, M. White, M. Whitten, J. Wood, C. Worthley, D. Wright, C. Yanari, L. Yeaman, D. Zempel, S. Zeppa.

NASA Ames Research Center (project management through 1989): W. Brooks, P. Davis, A. Dinger, L. Manning, R. Melugin, J. Murphy, R. Ramos, C. Wiltsee, F. Witteborn, L. Young.

NASA Headquarters (program management): N. Boggess, L. Caroff, B. Danchi, J. Frogel, J. Gardner, F. Gillett, J. Hayes, P. Hertz, D. Hudgins, W. Huntress, A. Kinney, L. LaPiana, W. B. Latter, K. Ledbetter, D. Leisawitz, K. MacGregor, J. Pajpayee, C. Pellerin, C. Scolise, K. Sheth, E. Smith, G. Stringfellow, H. Thronson, G. Wahlgren, K. Weaver, and E. Weiler

Smithsonian Astrophysical Observatory (Infrared Array Camera): **SAO (project management and science)**: L. Allen, C. Arabadjis, M. Ashby, P. Barmby, V. Bawdekar, J. Boczenowski, D. Boyd, J. Campbell-Cameron, J. Chappell, M. Cohen, K. Daigle, L. Deutsch, L. Frazier, T. Gauron, J. Gomes, J. Hora, M. Horan, J. Huang, J. Huchra, E. Johnston, M. Kanouse, S. Kleiner, D. Koch, M. Marengo, S. Megeath, G. Melnick, P. Okun, M. Pahre, B. Patten, J. Polizotti, J. Rosenberg, H. Smith, J. Spitzak, R. Taylor, E. Tollestrup, J. Wamback, Z. Wang, S. Willner; **NASA/ARC (Si:As detector array testing)**: J. Estrada, C. McCreight, M. McKelvey, R. McMurray, R. McHugh, N. Moss, W. Oglivie, N. Scott, S. Zins; **NASA/GSFC (instrument development)**: T. Ackerson, M. Alexander, C. Allen, R. Arendt, M. Armbruster, S. Babu, W. Barber, R. Barney, L. Bashar, C. Bearer, C. Bernabe, W. Blanco, R. Boyle, K. Brenneman, G. Brown, M. Brown, G. Cammarata, S. Casey, P. Chen, M. Cushman, P. Davila, M. Davis, M.

Dipirro, C. Doria-Warner, W. Eichhorn, D. Evans, D. Fixsen, J. Florez, J. Geiger, D. Gezari, D. Glenar, J. Golden, P. Gorog, S. Graham, C. Hakun, P. Haney, T. Hegerty, M. Jhabvala, F. Jones-Selden, R. Jungo, G. Karpati, R. Katz, R. Kichak, R. Koehler, R. Kolecki, D. Krebs, A. Kutyrev, J. Lander, M. Lander, N. Lee, J. Lohr, P. Losch, J. MacLoed, R. Maichle, S. Mann, N. Martin, P. Maymon, D. McComas, J. McDonnell, D. McHugh, J. Mills, C. Moiser, S. Moseley, T. Nguyen, T. Powers, K. Rehm, G. Reinhardt, J. Rivera, F. D. Robinson, C. Romano, M. Ryschkewitsch, S. Schwinger, K. Shakoorzadeh, P. Shu, N. Shukla, S. Smith, R. Stavely, W. Tallant, V. Torres, C. Trout, C. Trujillo, D. Vavra, G. Voellmer, V. Weyers, R. Whitley, J. Wolfgang, L. Workman, D. Yoder; **Raytheon Vision Systems (detector arrays)**: C. Anderson, J. Asbrock, V. Bowman, G. Chapman, E. Corrales, G. Domingo, A. Estrada, B. Fletcher, A. Hoffman, L. Lum, N. Lum, S. Morales, O. Moreno, H. Mosel-Riedo, J. Rosbeck, K. Schartz, M. Smith, S. Solomon, K. Sparkman, P. Villa, S. Woolaway; **University of Arizona**: W. Hoffman, T. Tysenn, P. Woida; **University of Rochester (InSb detector array testing)**: C. Bacon, R. Benson, H. Chen, J. Comparetta, N. Cowen, M. Drennan, W. Forrest, J. Garnett, B. Goss, S. Libonate, R. Madson, B. Marazus, K. McFadden, C. McMurtry, D. Myers, Z. Ninkov, R. Overbeck, J. Pipher, R. Sarkis, J. Schoenwald, B. White, J. Wu.

Spitzer Science Center, California Institute of Technology (science operations): W. Amaya, P. Appleton, D. Ardila, L. Armus, J. Aronsson, D. Avila, M. Barba, S. Barba, J. Bauer, R. Beck, C. Bennett, J. Bennett, B. Bhattacharya, M. Bicay, C. Bluehawk, S. Bonus, C. Boyles, H. Brandenburg, I. Bregman, C. Brinkworth, T. Brooke, J. Brauher, M. Burgdorf, S. Carey, M. Castillo, F. Cervantes, R. Chary, J. Chavez, W. Clavin, J. Colbert, D. Cole, S. Comeau, M. Crane, L. Dajose, D. Daou, A. Dean, V. Desai, M. Dobard, R. Ebert, R. Estrada, D. Fadda, S. Fajardo-Acosta, F. Fang, J. Fowler, D. Frayer, S. Freund, E. Furlan, L. Garcia, C. Gelino, W. Glaccum, T. Goldina, W. Green, T. Greene, C. Grillmair, E. Ha, E. Hacopians, A. Hadhazy, T. Handley, M. Harbut, B. Hartley, I. Heinrichsen, G. Helou, S. Hemple, D. Henderson, L. Hermans, T. Hesselroth, A. Hoac, D. Hoard, R. Hoban, J. Howell, H. Hu, H. Hurt, H. Huynh, M. Im, J. Ingalls, E. Jackson, J. Jacobson, T. Jarrett, G. Johnson-McGee, A. Kapadia, J. Keller, A. Kelly, E. Kennedy, I. Khan, D. Kirkpatrick, S. Kolhatkar, I. Kostadinova, J. Krick, M. Lacy, R. Laher, S. Laine, J. Lampert, J. Lampley, W. Latter, T. Lau, J. Lee, W. Lee, M. Legassie, D. Levine, J. Li, J. Llamas, T. Lo, W. Lockhart, L. Ly, P. Lowrance, N. Lu, J. Ma, W. Mahoney, D. Makovoz, V. Mannings, F. Marleau, T. Marston, F. Masci, H. McCallon, B. McCollum, D. McElroy, M. McElveney, N. McElveney, V. Meadows, Y. Mei, S. Milanian, K. Miller, A. Minamizaki, D. Mittman, A. Molloy, P. Morris, M. Moshir, A. Mulhall, R. Narron, B. Nelson, R. Newman, A. Noriega-Crespo, J. Ochotorena, P. Ogle, E. Oh, J. O'Linger, D. Padgett, R. Paladini, P. Patterson, A. Pearl, M. Pesenson, K. Phillips, S. Potts, T. Pyle, W. Reach, L. Rebull, J. Rector, J. Rho, T. Roberts, T. Roby, R. Rosen, C. Rosenthal, E. Ryan, R. Scholey, E. Scire, M. Seidel, S. Shenoy, K. Sheth, A. Shields, D. Shupe, N. Silbermann, L. Simurda, T. Soifer, I. Song, N. Sopata, G. Squires, J. Stauffer, S. Stierwalt, J. Stuesser, S. Stolovy, J. Surace, H. Teplitz, M. Thaller, G. Turek, S. Tyler, Z. Vainstein, S. Van Dyk, J. Vargas, L. Vu, S. Wachter, C. Waterson, W. Wheaton, S. Wheelock, J. White, A. Wiercigroch, G. Wilson, X. Wu, L. Yan, L. York, F. Yu.

University of Arizona (Multiband Imaging Photometer for Spitzer): **Arizona (project management, array construction, and science)**: A. Alonso-Herrero, M. Alwardi, I. Barg, M. Blaylock, M. Bradley, M. Buglewicz, J. Cadien, A. Churchill, H. Dang, L. Davidson, J. T. Davis, H. Dole, E. Egami, C. Engelbracht, K. A. Ennico, J. Facio, J. Flores, K. D. Gordon, L. Hammond, D. Hines, J. Hinz, R. Hodge, T. Horne, P. Hubbard, D. M. Kelly, D. Knight, K. A. Kormos, E. LeFloc'h, F. J. Low, M. McCormick, T. J. McMahon, T. Milner, K. Misselt, J. Morrison, K. Morse, J. Muzerolle, G. X. Neugebauer, L. Norvelle, C. Papovich, P. Perez-Gonzalez, M. J. Rieke, G. Rivlis, P. Rogers, R. Schnurr, M. Scutero, C. Siqueiros, P. Smith, J. A. Stansberry, P. Strittmatter, K. Su, C. Thompson, P. van Buren, S. Warner, K. White, D. A. Wilson, G. S.

Winters, E. Young; **University of California Berkeley/LBNL (science and detector material)**: E. Arens, J. W. Beeman, E. E. Haller, P. L. Richards; **Jet Propulsion Laboratory (science)**: C. Beichman, K. Stapelfeldt; **National Optical Astronomy Observatories (science)**: J. Mould; **Center for Astrophysics (science)**: C. Lada; **Ball Aerospace (instrument development)**: D. Bean, M. Belton, T. Bunting, W. Burmester, S. Castro, C. Conger, L. Derouin, C. Downey, B. Frank, H. Garner, P. Gentry, T. Glenn, M. Hegge, G. B. Heim, M. L. Henderson, F. Lawson, K. MacFeely, B. McGilvray, R. Manning, D. Michika, C. D. Miller, D. Morgan, M. Neitenbach, R. Novaria, R. Ordonez, R. J. Pearson, Bruce Pett, K. Rogers, J. P. Schwenker, K. Shelley, S. Siewert, D. W. Strecker, S. Tennant, J. Troeltzsch, B. Unruh, R. M. Warden, J. Wedlake, N. Werholz, J. Winghart, R. Woodruff, C. Yanoski; **Raytheon (readout development)**: J. Asbrock, A. Hoffmann, N. Lum; **Ames Research Center (readout development)**: C. McCreight; **QM Industries (far-infrared filters)**: P. A. R. Ade; **Blackforest Engineering (engineering support)**: S. Gaalema; **Battel Engineering (engineering support)**: S. Battel; **SRON (scan mirror development)**: T. Degraauw

Appendix D. List of Figures

Appendix E. List of Tables

Appendix F. Index